CANADA

DEPARTMENT OF ENERGY, MINES AND RESOURCES

OTTAWA

MINES BRANCH INVESTIGATION REPORT IR 67-56

FERRITES: PART 1. LITERATURE SURVEY ON PERMANENT-MAGNET-TYPE FERRITE TECHNOLOGY

by

SUTARNO AND W. S. BOWMAN

MINERAL SCIENCES DIVISION

D. R. B. PROJECT D48-55-01-21

E. C. R. D. C. - C. 73

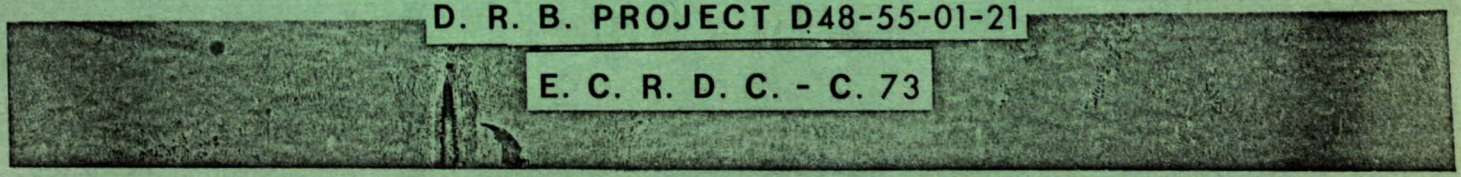

COPY NO.

AUGUST 10, 1967

Mines Branch Investigation Report IR 67-56

FERRITES: PART I. LITERATURE SURVEY ON PERMANENT-MAGNET-TYPE FERRITE TECHNOLOGY

by

Sutarno* and W. S. Bowman**

- - -

SUMMARY

A survey of earlier work on permanent-magnet type ferrites with the nominal composition of (Ba, Sr, Pb)O. $6 \cdot 0 Fe_2O_3$ is given, mainly from the technological point of view. The discussion includes a consideration of the phase relations, crystal structure, magnetic properties, method of preparation and other factors affecting the finished product.

---

*Research Scientist and **Technical Officer, respectively, Physical Chemistry Section, Mineral Sciences Division, Mines Branch, Department of Energy, Mines and Resources, Ottawa, Canada.

CONTENTS

- - - -

INTRODUCTION

The discovery that ceramic materials fabricated from a certain group of ferrite-based compounds could be used as permanent-magnet devices was made in the nineteen-thirties (1)*. These compounds have a hexagonal structure with strong magnetic anisotropy, with easy magnetization in some cases in the direction of, and, in others, perpendicular to, the c-axis. The compounds under investigation in the present programme have easy magnetization along the direction of the c-axis. These compounds are commonly referred to as the "M" compounds. The ideal composition of such materials has been stated to be $MO.6{\cdot}0Fe_2O_3$, where M = Ba, Sr, Pb or a mixture thereof.

In the early days, there was little interest in any practical applications of these materials because of the low value of their energy product, $(BH)_{max}$, which was about 1 MGOe (mega-gauss-oersted), much lower than that of metallic magnets. After the Second World War, this value was successfully improved mainly by inducing the particles in the body to take up a crystallographically unidirectional orientation, thus taking full advantage of the crystal anisotropy of the ferrite compounds. Other factors that affect the $(BH)_{max}$ value are the chemical composition and the conditions of ceramic processing.

At present, "hard" ferrite-based magnets with energy products as high as 4.8 MGOe at an intrinsic coercive force of iH_c = 2.4 kOe, to $(BH)_{max}$ = 0.8 MGOe at iH_c = 11 kOe, have been reported (2). These ferrites have a composition based on $SrO.6{\cdot}0Fe_2O_3$ with some sulphate additives in them. Besides having a high energy product, strontium ferrite also has the advantage of being lighter in weight than the corresponding barium-based compound.

In this programme (3), (Ba, Sr, Pb)$O.nFe_2O_3$, possibly with some additives, are being investigated. This report is a summary of the literature published up to the present on ferrite-based permanent-magnetic materials dealing mainly with the technological aspects of the work.

---

*For references, see pages 40-42.

CHEMISTRY AND CRYSTAL STRUCTURE OF HEXAGONAL FERRITES

1. Chemical Composition of Hexagonal Ferrites

Ferrite compounds of the type under consideration have closely related hexagonal structures and can be represented in the phase diagram illustrated in Figure 1.

Compounds M, W, Y, Z and others (which are combinations of these) have very closely related hexagonal structures. They all have a strongly anisotropic magnetization. Some of these compounds, including the M compound, have their easy directions of magnetization along the c-axis, while others, like the Y compound, have an easy planar magnetization perpendicular to the c-axis. At present, only the M compounds will be investigated in this programme, and, in the remainder of this report, the word "ferrite" will be taken to refer to the M compound only, unless it is stated otherwise. The Ba in this type of compound can be replaced in part or completely by Sr or Pb, and in part by Ca and certain rare-earth ions.

The common method of ferrite preparation is to react iron oxide (or any compound that will produce iron oxide upon heating) with suitable Ba, Sr or Pb compounds. During this reaction, intermediate products are formed. In order to be able to identify these various intermediate products, a knowledge of the $MO\text{-}Fe_2O_3$ systems (where M = Ba, Sr or Pb) is essential. Goto and Takada (4) have investigated part of the barium oxide-iron oxide system. Their phase diagram is reproduced in Figure 2. Mountvala and Ravitz (5) have studied part of lead oxide-iron oxide system, and their results are shown in Figure 3.

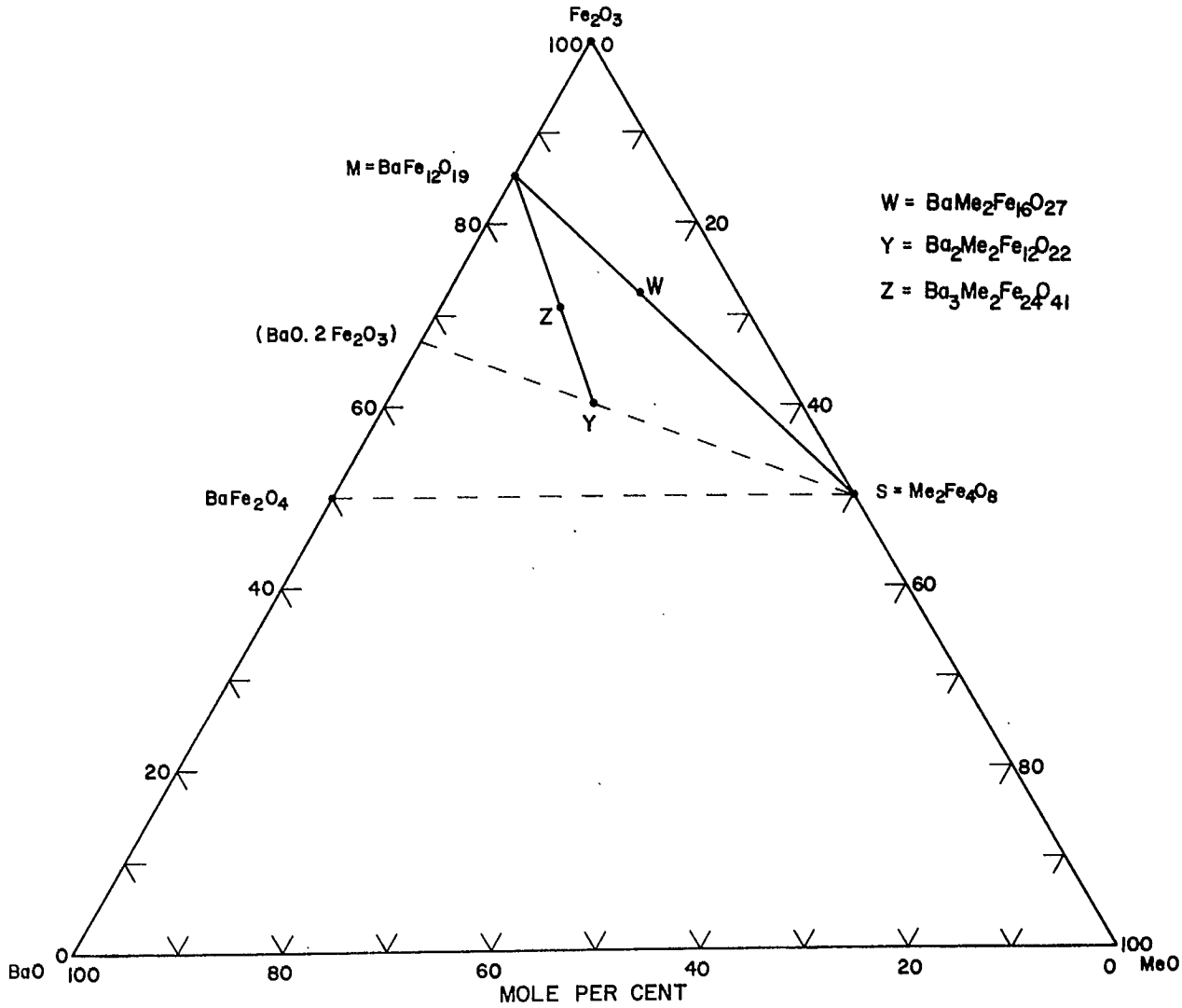

Figure 1. Compositional Diagram for the Ferromagnetic Ferrites, reproduced from Reference (10). (Me = a divalent ion)

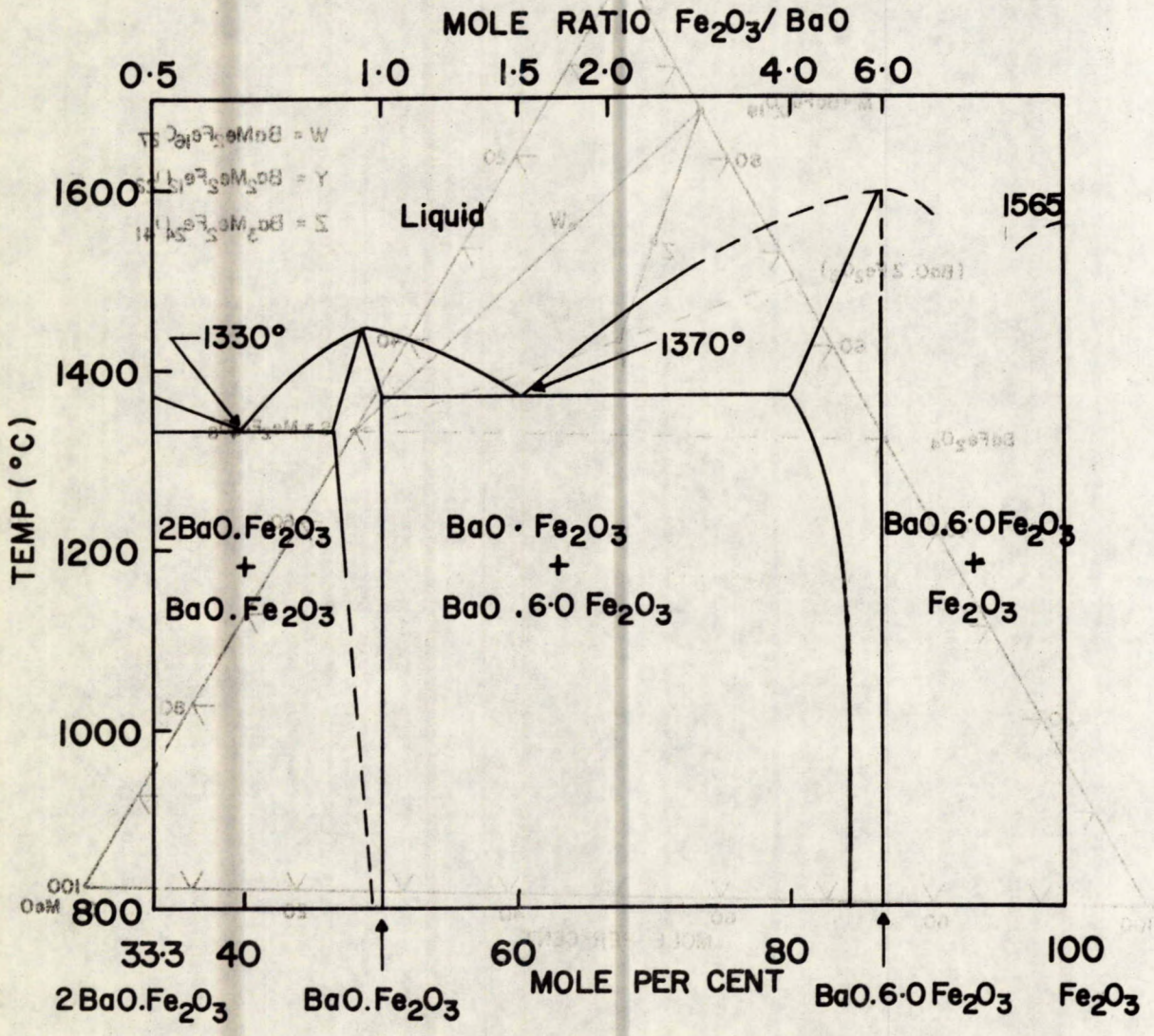

Figure 2. The System $2BaO.Fe_2O_3$-Fe_2O_3, reproduced from Yasumasa Goto and Toshio Takada, Journ. Amer. Ceram. Soc., 43 [3] 151 (1960).

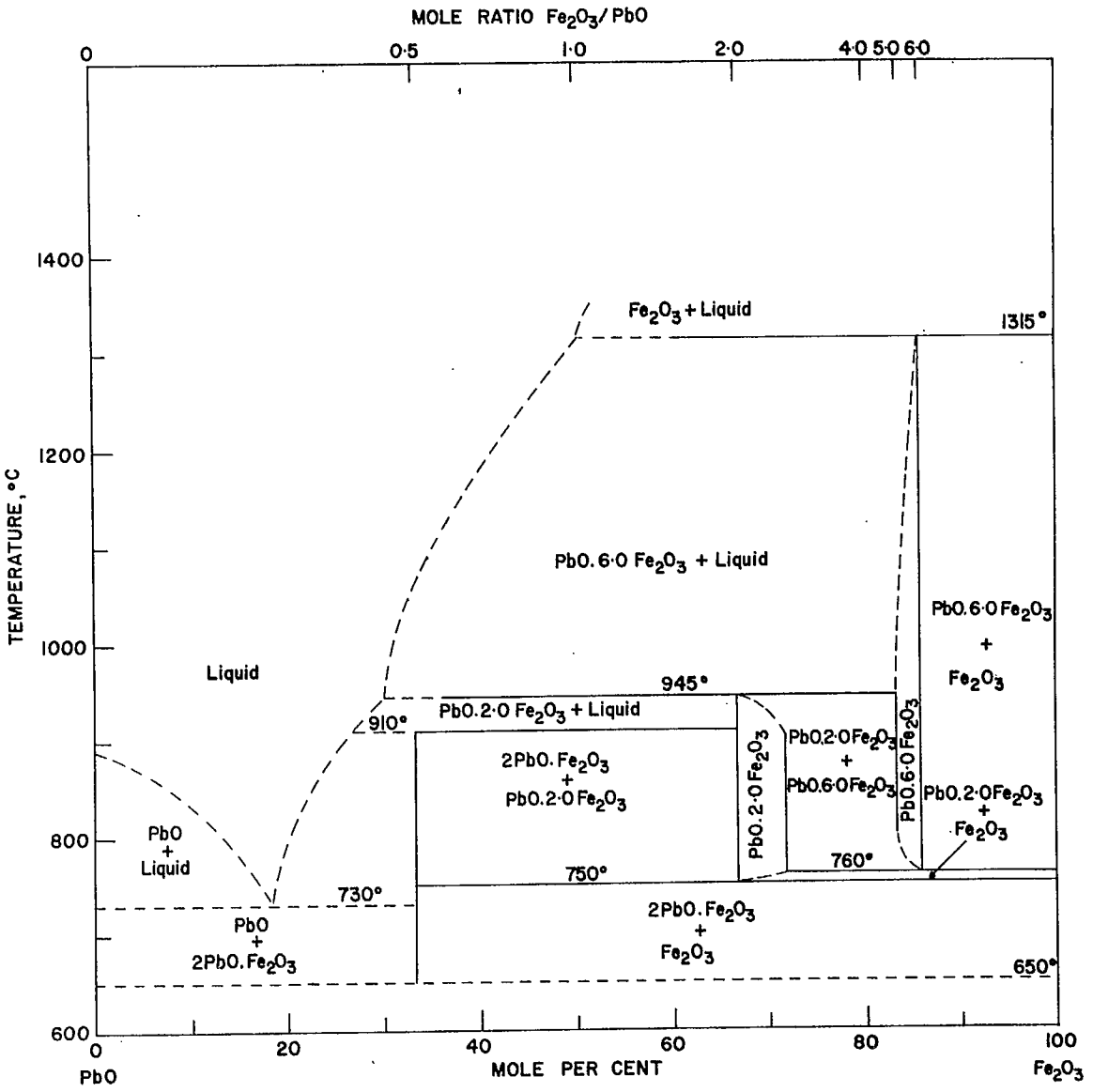

Figure 3. The System PbO-Fe_2O_3, reproduced from A.J. Mountvala and S.F. Ravitz, Journ. Amer. Ceram. Soc., 45 [6], 286 (1962).

2. Crystal Structure of the M Compound

It is widely accepted that the M compound is isostructural with the mineral magnetoplumbite, as reported by Adelsköld (6). The structure is hexagonal with the space group $P6_3/mmc$-D^4_{6h}; each unit cell contains two formula units.

The atoms are situated in the following positions (7, 8):

Ba	(2d) :	2/3, 1/3, 1/4, etc.
Fe	(2a) :	0 , 0 , 0
	(2b) :	0 , 0 , 1/4,
	(4f) :	1/3, 2/3, Z_{Fe1}
	(4f) :	1/3, 2/3, Z_{Fe2}
	(12k) :	1/6, 1/3, Z_{Fe3}
O	(4e) :	0 , 0 , Z_{O1}
	(4f) :	1/6, 1/3, Z_{O2}
	(12k) :	1/6, 1/3, Z_{O3}
	(12k) :	1/2, 0 , Z_{O4}

The lattice constants of barium ferrite and the related compounds are listed in Table 1.

TABLE 1

Lattice Constants of Barium Ferrite and Related Compounds (8)

Compound	a_o(Å)	c_o(Å)
$BaO.6\cdot0Fe_2O_3$	5.888	23.22
$SrO.6\cdot0Fe_2O_3$	5.876	23.08
$PbO.6\cdot0Fe_2O_3$	5.889	23.07
$K_2O.11\cdot0Fe_2O_3$	5.927	23.73
$Rb_2O.11\cdot0Fe_2O_3$	5.927	23.88
$BaO.6\cdot0Al_2O_3$	5.588	22.22
$SrO.6\cdot0Al_2O_3$	5.568	21.99
$CaO.6\cdot0Al_2O_3$	5.547	21.87
$K_2O.11\cdot0Al_2O_3$	5.598	22.71
$Na_2O.11\cdot0Al_2O_3$	5.595	22.49

The structure of $(Na,K)_2O.11\cdot0Fe_2O_3$ is almost the same as that of $(Ba,Sr,Pb)O.6\cdot0Fe_2O_3$, except that in the former compound, there are metal vacancies in the (2b) positions and oxygen vacancies in the (6h) positions; also, there are two additional oxygen atoms occupying (2c) positions.

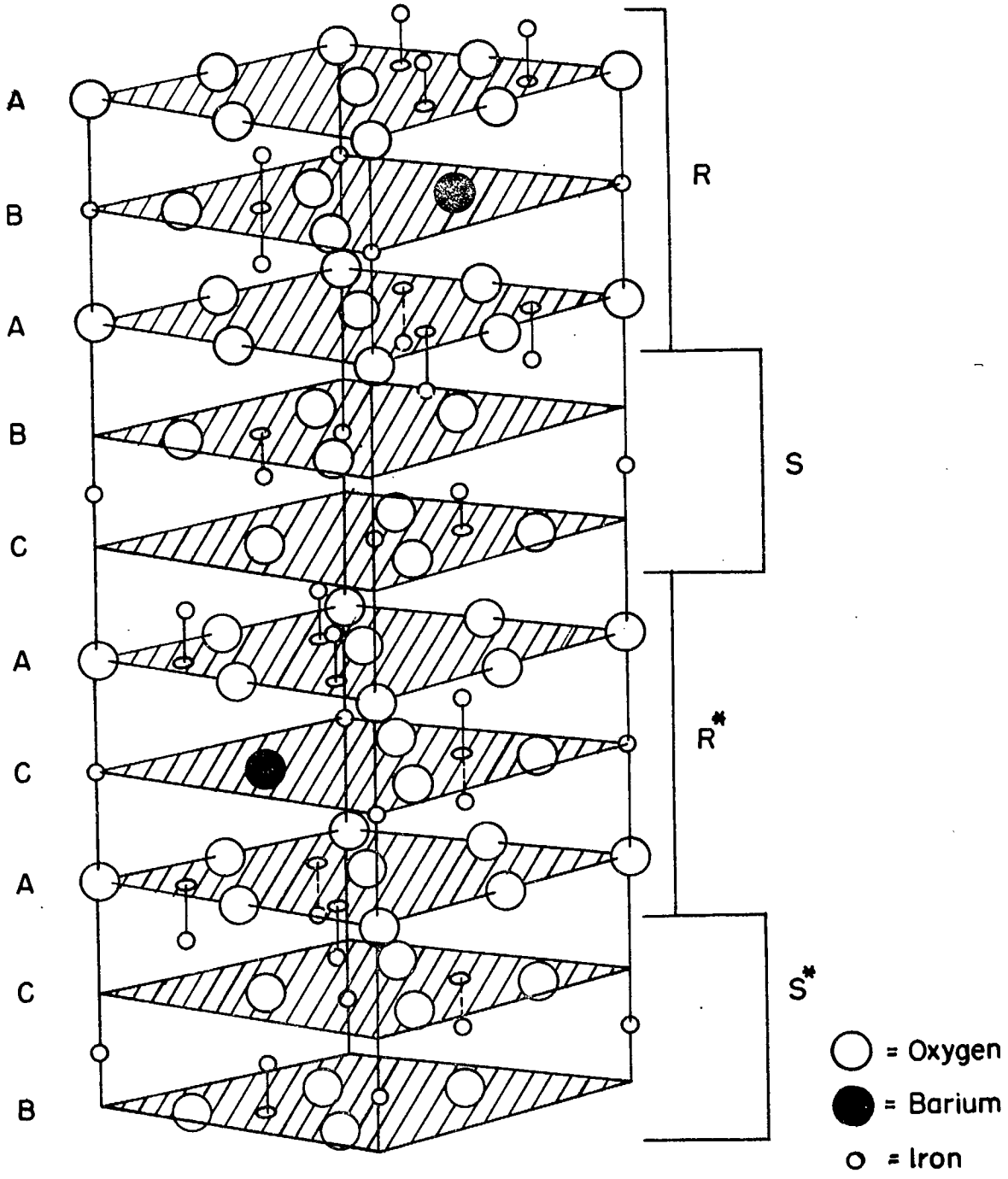

Figure 4. Crystal Structure of the M Compound (1 unit cell).

The crystal structure of the M compound, as illustrated in Figure 4, is composed of hexagonally and cubically close-packed oxygen-ion units. The hexagonal close-packed structure is shown in Figure 5(I). The centres of the oxygen ions B lie in a horizontal plane and form equilateral triangles. The oxygen ions A are also close-packed and are in a layer above the B layer. There is another layer of oxygen ions below the B layer whose centres lie vertically below those ions in the A layer. Below this layer, there is another layer whose centres lie vertically below those ions in the B layer. Continuing in the vertical direction, we thus obtain the sequence of layers ABABABA---. This sequence produces a uniaxial hexagonal crystal structure in which the c-axis is perpendicular to the oxygen layers.

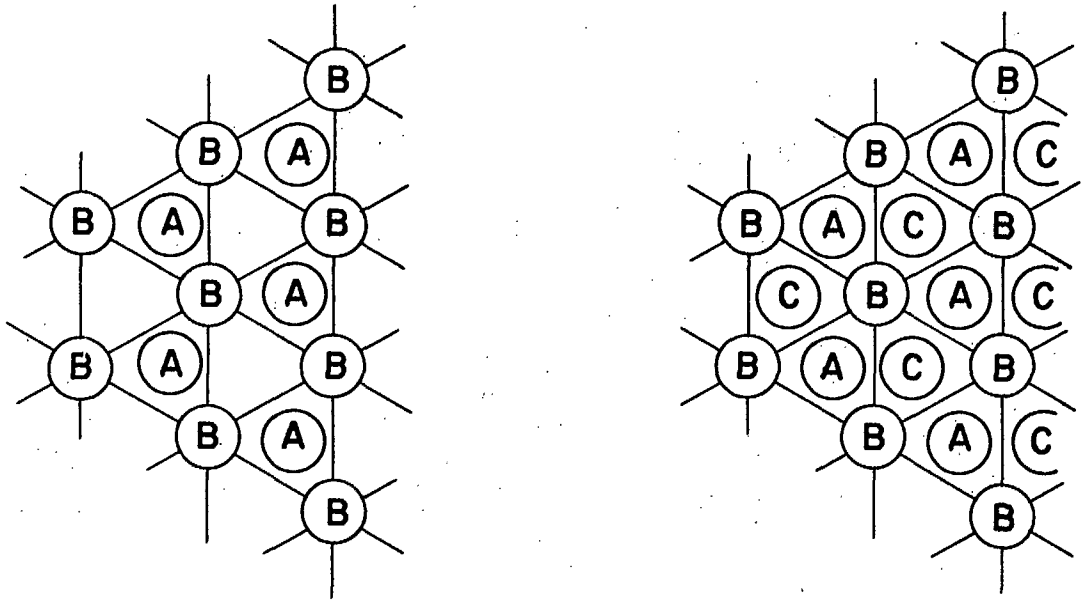

I II

Figure 5. Schematic Diagram of: I - Close-packed Hexagonal Structure.
II - Close-packed Cubic Structure.

The cubic close-packed structure is shown in Figure 5(II). The sequence of layers is ABCABCA---, where the oxygen ions A and B have the same positions as in Figure 5(I), and the oxygen ions C are close-packed in a layer the same distance below the B layer as the A layer is above it. Obviously, the sequences ACBACBA--- and ACACACA--- also give rise to cubic and hexagonal crystal structures, respectively.

In the M compound, the layers containing barium (which replaces one of the oxygens) are hexagonally packed with respect to the two adjacent oxygen layers. The four oxygen layers between those containing barium are cubically close-packed. There is, thus, an overlap of cubically and hexagonally close-packed sections of the structure, which is possible because the two sections are built up from the same type of oxygen layers.

The M compound can be considered to be composed of two kinds of blocks. The first type of block, which is commonly called the S block, consists of two layers of cubically close-packed oxygen ions with the iron ions occupying the interstitial positions in the same manner as those in the spinel structure. The [111] direction of the spinel lattice is directed along the c-axis of the hexagonal lattice. This block contains two formula units of Fe_3O_4. Four of the cations reside in octahedral sites and contribute to the magnetic moment of the majority (α) sub-lattice. The other two cations are tetrahedrally co-ordinated and contribute to the minority (β) sub-lattice. If all the cations are Fe^{3+}, the S block makes a net contribution of two ferric magnetic moments, which is 10 Bohr magnetons, to the majority sub-lattice.

The second type of block, usually called the R block, consists of three layers of hexagonally close-packed oxygen ions with the iron ions located interstitially. The middle layer, which is a mirror plane, has one of the oxygen ions replaced by a barium. To balance the charge, the two Fe^{2+} that would otherwise reside immediately above and below the replaced oxygen are also absent.

The barium ions are thus co-ordinated by twelve oxygens. This block is devoid of tetrahedral cations, but contains five octahedral cations. Three of these lie on the boundary, and one lies half way between each pair of oxygen layers (these cations lie on a threefold axis). The remaining cation lies in the middle oxygen plane in a novel interstice with five-fold oxygen co-ordination. It is noteworthy that the close-packed oxygen radius, which is 1.32 Å, is such that the hole for this latter iron position is too small for the radius of Fe^{3+}. The three bounding octahedral ions and the trigonal ion contribute to the majority sub-lattice. The two octahedral ions adjacent to the Ba-plane contribute to the minority sub-lattice. If all the cations are Fe^{3+}, as in the S block, then the R block would make a net contribution of two ferric magnetic moments, which is 10 Bohr magnetons, to the majority sub-lattice. The formula unit of this block is $BaFe_6O_{10}$.

The blocks are combined in such a way that the sequence is RSR*S*RSR*S*R---, where R* and S* are identical to the R and S blocks except that they are rotated through 180° about the c-axis. Hence the layers containing barium are mirror planes. The sequence of layers in the M structure is, therefore, $\underbrace{\text{ABABCACACBABA}}_{\text{unit cell}}$---, since the B layer becomes identical to the C layer and vice versa when rotated through 180°. The unit cell, therefore, contains two formula units and consists of ten close-packed oxygen layers.

MAGNETIC PROPERTIES OF FERRITE-BASED MAGNETS

Some of the properties of M-compound-based magnets are directly affected by their method of preparation. Certain of such properties will be discussed in this report.

1. Saturation Magnetization

The magnetic moment of the M compound can be illustrated in the following table:

TABLE 2

Cation Distribution of the M Compound

Block	Formula	Cation Distribution and Spin Direction			
		Tetrahedral	Octahedral	Trigonal	Net
S	Fe_6O_8	2↓	4↑	-	2↑
R	$BaFe_6O_{11}$	-	3↑ 2↓	1↑	2↑
Total	$BaFe_{12}O_{19}$	2↓	7↑ 2↓	1↑	4↑

The total net magnetic moment is that of 4 cations with parallel spins. If all these cations are Fe^{3+}, then the total magnetic moment per formula unit will be 20 Bohr magnetons. This value is in agreement with the experimental value reported by Stuijts (9). He measured the saturation magnetization of polycrystalline barium hexaferrite at liquid hydrogen temperatures with an applied field of up to 26,000 Oe. The highest reported saturation magnetization for this ferrite at 20°C is 4775 gauss (10) and for strontium ferrite, 4652 gauss. Figure 6 shows the saturation magnetization as a function of temperature for barium and lead ferrites, reproduced from references (10) and (11). The saturation magnetization depends only on the purity and structure of the material, the temperature and the sintered density.

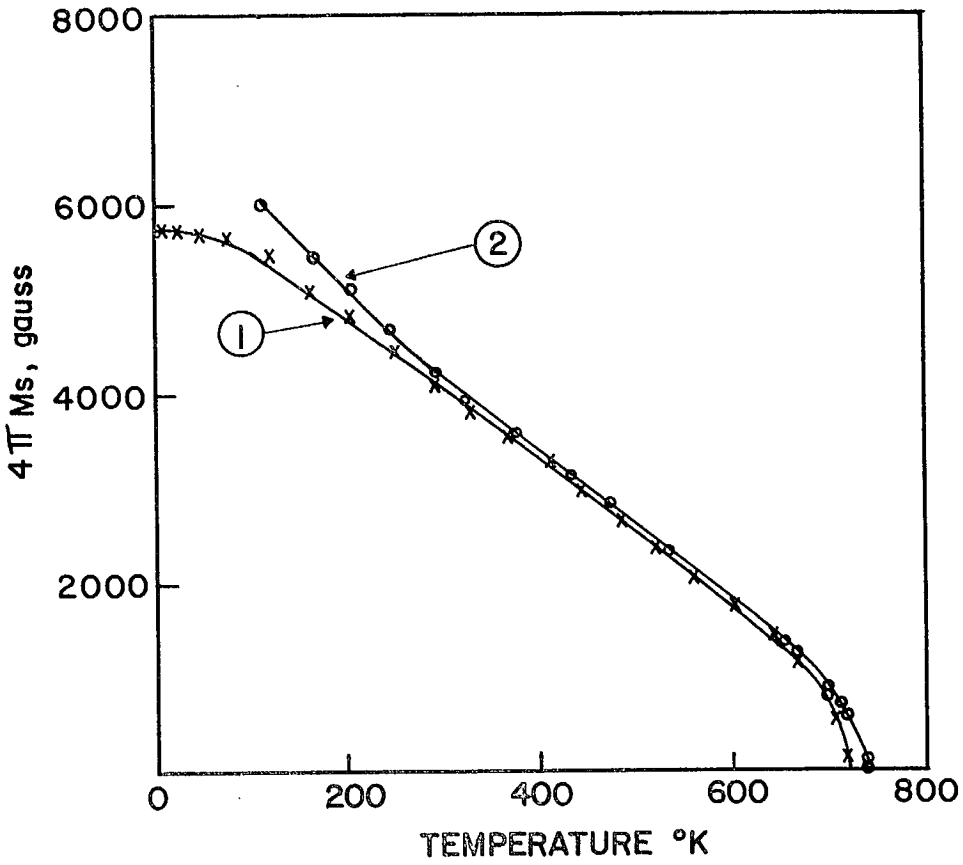

Figure 6. Saturation Magnetization vs. Temperature, for (1) Lead Ferrite, (2) Barium Ferrite, reproduced from R. Pauthenet and G. Rimet, C.R. Acad. Sci., 249, (1959) p. 1875; and J.J. Went et al., Phil. Tech. Rev., 86, (1952), p. 424, respectively.

2. Magnetic Anisotropy

One of the most valuable properties of this type of ferrite from the point of view of its use as a permanent-magnet material is its magnetic anisotropy.

The anisotropic energy of a hexagonal crystal (10) can be expressed as:

$$E_k = K_1 \sin^2 \alpha + K_2 \sin^4 \alpha + K_3 \sin^6 \alpha + \text{---} \quad \ldots \text{(Eq. 1)}$$

where: E_k = Crystal anisotropic energy,

K_1, K_2 and K_3 = Anisotropic constants,

and α = the angle between the direction of magnetization and the c-axis.

If all but the first term are neglected, the easy magnetization will depend on the value of K_1. If $K_1 > 0$, the easy direction lies along the c-axis, whereas for $K_1 < 0$, the easy direction lies in the plane perpendicular to the c-axis.

For an illustration of this point, consider Figure 7. H is the applied field at an angle α_o from the c-axis; M_s is the magnetic vector of the crystal at equilibrium at an angle α from the c-axis.

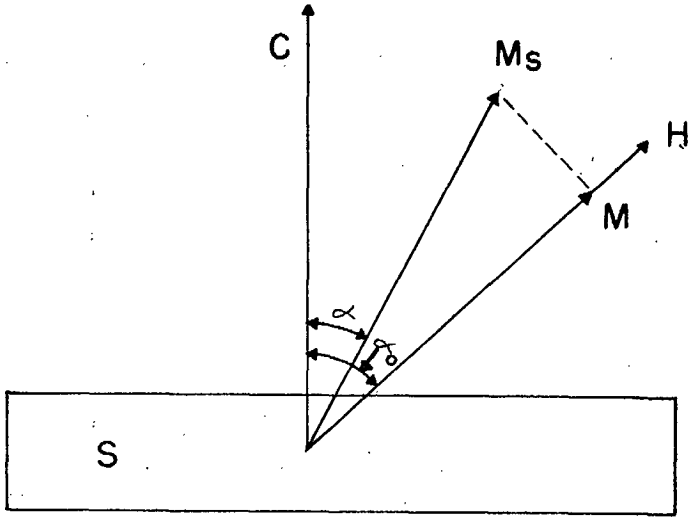

Figure 7. Schematic diagram of the single-domain magnetization process.

According to the domain theory, a single-domain particle, in the absence of an external magnetic field, will have its magnetization M_s directed in the preferred direction (in this case the c-axis). When an external magnetic field H is applied to the particle at an angle α_o with respect to the c-axis, then the direction of M_s will turn away from the c-axis toward the direction of H. In the equilibrium condition, the magnetization M_s will

make an angle α with respect to the c-axis. The value of α depends on the magnitude and the direction of H and also on the anisotropic energy of the particle. This angle can be calculated by minimizing with respect to the angle α the total energy, which is composed of the crystal-anisotropy energy E_k and the energy of the interaction between magnetization M_s and field H.

The total energy E can be expressed as:

$$E = E_k - H M_s \cos(\alpha_o - \alpha) \quad \ldots \text{(Eq. 2)}$$

Neglecting all other terms but the first term for E_k, the above equation can be expressed as:

$$E = K_1 \sin^2 \alpha - H M_s \cos(\alpha_o - \alpha) \quad \ldots \text{(Eq. 3)}$$

E will be a minimum when $\partial E/\partial \alpha = 0$;

$$\text{i.e. when } K_1 \sin 2\alpha - H M_s \sin(\alpha_o - \alpha) = 0 \quad \ldots \text{(Eq. 4)}$$

$$\text{or when } H = \frac{K_1 \sin 2\alpha}{M_s \sin(\alpha_o - \alpha)} \quad \ldots \text{(Eq. 5)}$$

Thus, given the magnitude and the direction of H with respect to the c-axis (angle α_o), the angle α can be computed.

Hence, when H is applied and before the particle rotates, the magnetization M (in the direction of H) is

$$M = M_s \cos(\alpha_o - \alpha) \quad \ldots \text{(Eq. 6)}$$

For the field in a direction perpendicular to the c-axis ($\alpha_o = 90°$),

$$H = \frac{K_1 \sin 2\alpha}{M_s \sin(90 - \alpha)} \quad \ldots \text{(Eq. 7)}$$

$$\text{or} \quad H = \frac{2K_1 \sin \alpha}{M_s} \quad \ldots \text{(Eq. 8)}$$

$$\text{and} \quad \sin \alpha = \frac{H}{H_a}$$

where $H_a = \frac{2K_1}{M_s}$ is called anisotropic field, the field required to turn the magnetization vector 90° from its preferred direction.

Since both K_1 and M_s are temperature-dependent, H_a must also be temperature-dependent. Fortunately, at temperatures up to about 425°K, H_a does not change very rapidly with temperature. For barium hexaferrite in this temperature region, H_a is of the order of 17,000 Oersteds. The values of K_1, H_a and $4\pi M_s$ as a function of temperature have been reported by Casimir et al. (12), and are reproduced in Figure 8.

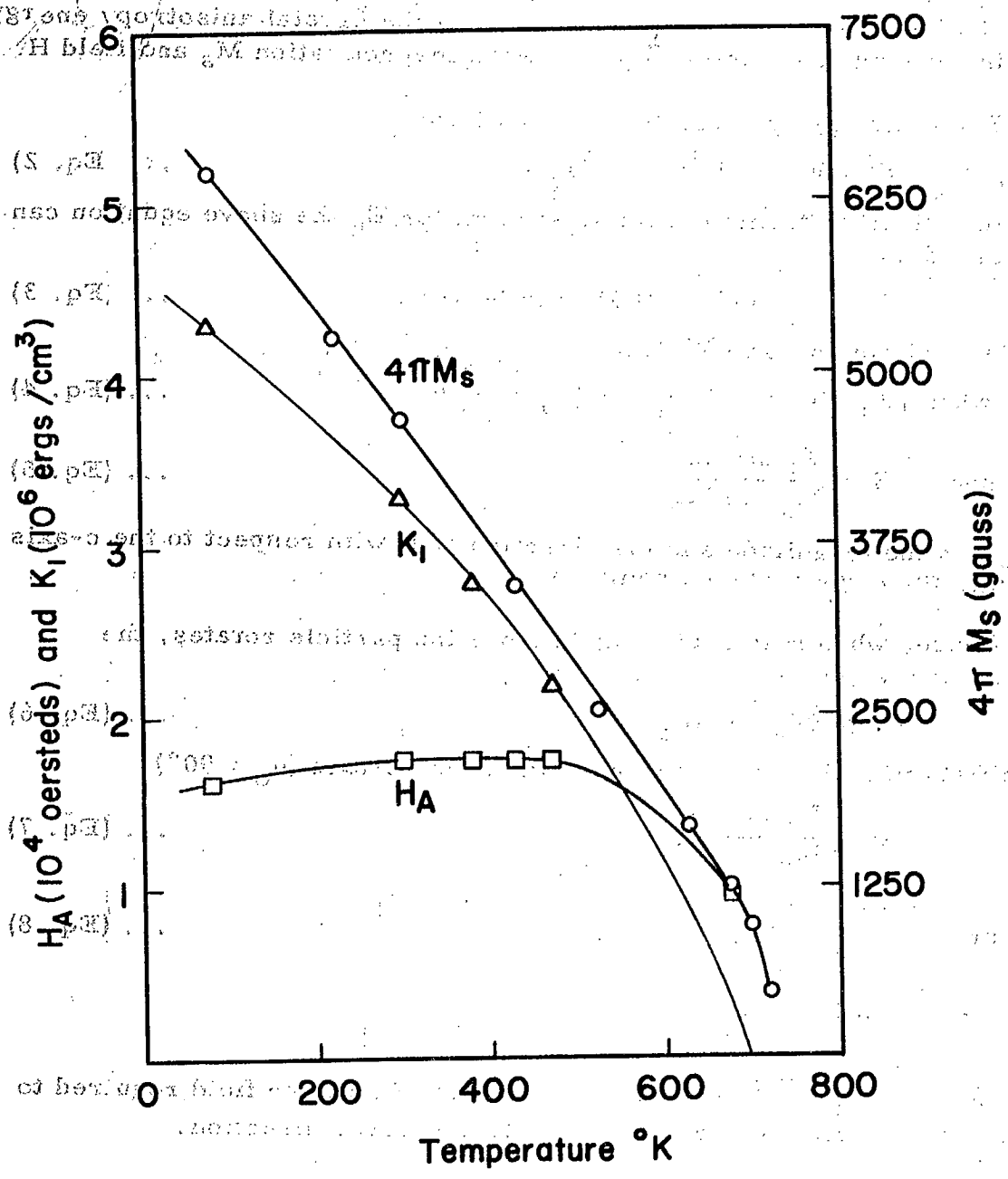

Figure 8. Anisotropic Constant, Anisotropy Field and Saturation Magnetization of Barium Ferrite as a Function of Temperature (reproduced from Ref. 12).

3. Energy Product, (BH)

A given volume of magnetic material will produce the highest field in a given air space when the induction B in the material is such that the energy product BH is a maximum.

Consider the ring magnet of Figure 9, in which L_s, A_s and L_g, A_g are the lengths and cross-sectional areas of the specimen and air gap, respectively.

Since there is no external field, the demagnetization integral

$$\oint H \, dL = 0 \qquad \ldots \text{(Eq. 9)}$$

when the integral is taken around the closed path, including the air gap.

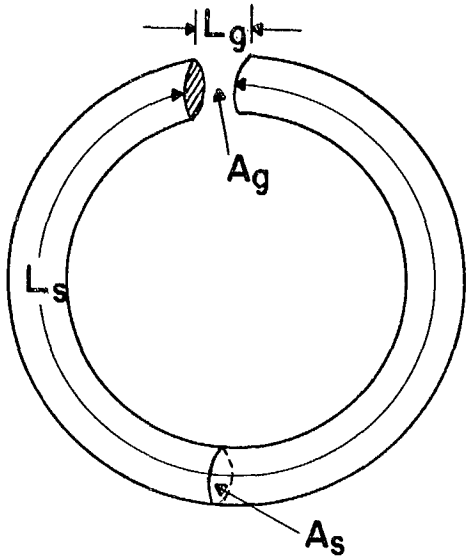

Figure 9. Schematic diagram of a magnetic circuit with an air gap.

If H and B are the field strength and induction, respectively, of the specimen and H_g is the field strength in the air gap, and, if they are assumed to be constant, the above integral can be simplified to:

$$H L_s + H_g L_g = 0 \qquad \ldots \text{(Eq. 10)}$$

and, since the flux lines are continuous,

$$H_g A_g = B A_s \qquad \ldots \text{(Eq. 11)}$$

The above relations combine to give:

$$H_g^2 = -B H (V_s/V_g) \qquad \ldots \text{(Eq. 12)}$$

where V_s and V_g are the volumes of the gap and the specimen, respectively. Thus, H_g is a maximum when B H is a maximum for a given volume ratio. The value of $(BH)_{max}$, which is commonly called the energy product, is used to determine the merit of a permanent magnet.

4. Demagnetization Curve

Most magnetic circuits containing a magnet also include an air gap. Consequently, the magnet usually operates under the influence of a demagnetizing field and hence, not at its residual magnetization but at a value lower than B_r. Thus, the important curve for a permanent-magnet material is that portion of the hysteresis loop that lies in the second quadrant, of the B-H graph between the residual induction and the coercive force. This is called the demagnetization curve.

In order to increase the value of $(BH)_{max}$, besides having to increase the values of the residual induction, B_r and of the coercive force, H_c (Figure 10), the squareness of the demagnetization curve must also be increased. This squareness is expressed as a quantity γ (13), which is sometimes called the fullness factor, and is defined as:

$$\gamma = \frac{(BH)_{max}}{B_r . iH_c} \qquad \ldots \text{(Eq. 13)}$$

Theoretically, γ must lie between 0.25 for a linear demagnetization curve and 1.0 for a completely square curve.

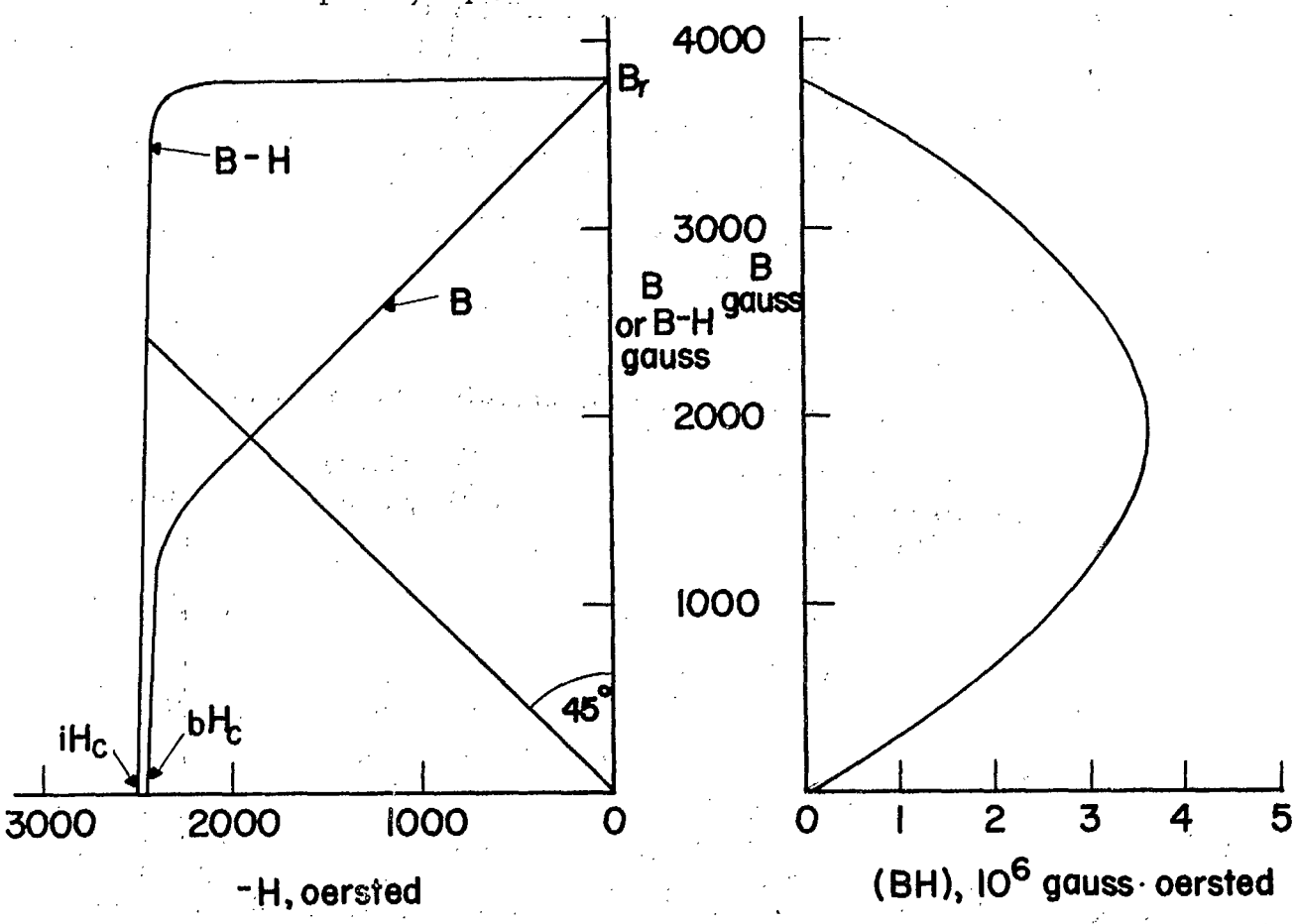

Figure 10. Typical demagnetization and (BH) curve for a ferromagnetic material.

CRYSTAL ORIENTATION

1. Principle of Orientation

It has been mentioned in an earlier section of this report that the usefulness of this type of ferrite as a basic material for permanent magnets is mainly due to its strong crystal anisotropy. The energy product of a piece of magnet can be improved by increasing its coercive force, its residual magnetization and the squareness of its demagnetization curve. The residual magnetization, for a given anisotropic material with a certain saturation magnetization value, depends on the orientation of its crystals with respect to the magnetic direction of the body. This dependence is illustrated in Figure 11.

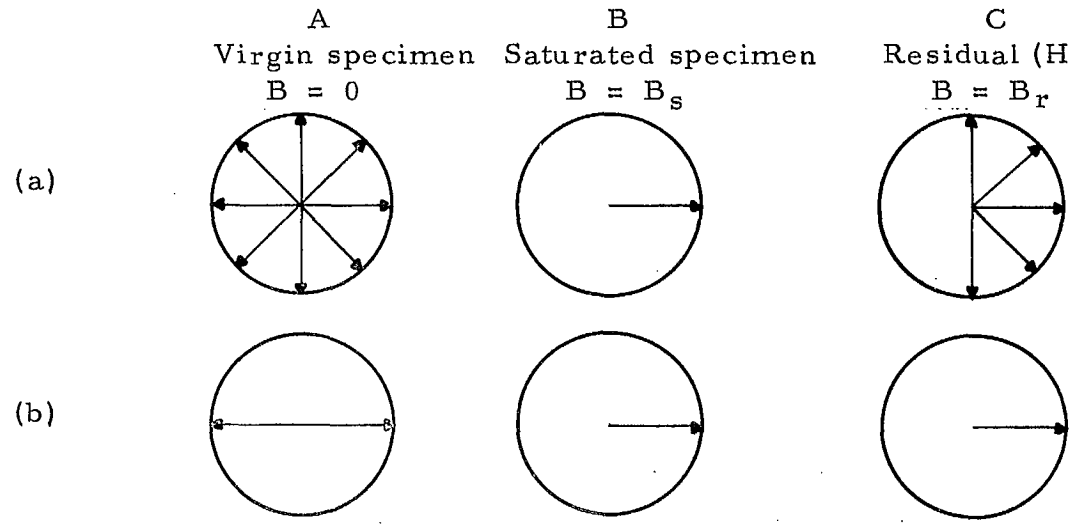

Figure 11. Schematic diagram of domain orientation in a ferrite permanent-magnet specimen: (a) = random specimen and (b) = oriented specimen.

Figure 11 shows the schematic diagram of the domain orientation within the specimen at various stages. Figure 11 (a) shows the situation in a completely-randomly-oriented specimen. Before this specimen is magnetized (A), the domain orientation has the same probability for any direction. At the saturation point (B), all the domains are oriented in the direction of the field H. When H is reduced to 0, the anisotropic spring will pull the directions of these domains into their preferred directions, but only to occupy half of the circle (C) instead of going back to their original orientations (A). From this diagram, it can be computed that, in a random specimen:

$$\frac{M_r}{M_s} = 1/2\pi \int_0^{\pi/2} 2\pi \sin\alpha \cos\alpha \, d\alpha = 0.5 \qquad \ldots \text{(Eq. 14)}$$

where $4\pi M = (B-H)$ is the magnetization, and the subscripts r and s indicate remanent and saturation respectively, and α is the angle between the local magnetization and the field. Figure 11(b) represents a fully-oriented specimen. All crystals are oriented in the same direction. When the specimen is virgin (A), the probability that the domains are directly towards the two opposite directions is equal. The resultant of magnetization is, therefore, zero. When the specimen is saturated (B), all the domains are directed towards the direction of H. The field required to saturate this specimen is very small compared with that required for specimen (a), since there is no anisotropic spring to overcome. This field is of the magnitude of the coercive force. When the external field H is reduced to zero, the direction of all the domains remains the same since they are already in their preferred direction (C). From this diagram is can be seen that, for oriented specimens, the ratio

$$\frac{M_r}{M_s} = 1.0$$

Figure 11, of course, represents ideal conditions. In practice, the M_r/M_s ratio for oriented specimens is about 0.96 (14). Therefore, by orienting the specimen, M_r is increased by up to 100 per cent.

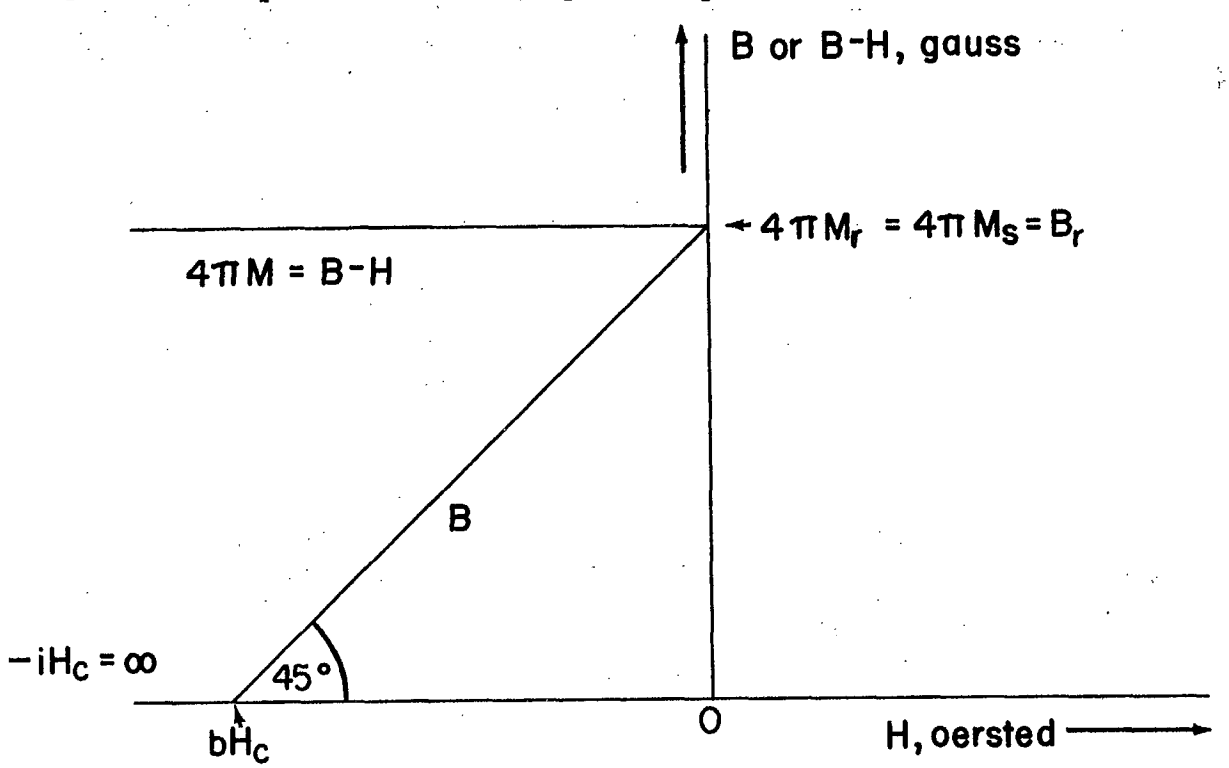

Figure 12. Demagnetization curve for an ideal magnet with infinite coercive force.

As is shown in Figure 12, for an ideal magnet with infinite intrinsic coercive force ($iH_c = \infty$), the energy product is given by

$$(BH)_{max} = (B_r/2)^2 \qquad \ldots \text{(Eq.15)}$$

Thus, for this material, orientation will increase its energy product by a factor of 4. For $BaO.6 \cdot 0 Fe_2O_3$ at room temperature, $4\pi M_s = 4775$ gauss; ideally, then,

$$(BH)_{max} = (4775/2)^2 = 5.7 \times 10^6 \text{ G.Oe.}$$

In practice, however, the $(BH)_{max}$ obtained is much lower.

A drawback of this orientation is that it promotes the formation of Weiss domains, owing to the fact that the preferred directions of magnetization (the c-axis) in adjacent grains have approximately the same orientation, so that the Weiss domain can easily continue from one crystal to another and there is, thus, a danger that the graininess of the material, which should be the reason for the absence of domain walls, will be lost. A high residual magnetization is, thus, associated with a low coercive force (10). The highest reported $(BH)_{max}$ value so far obtained is 4.8×10^6 G.Oe. for a strontium-based ferrite magnet (2).

2. Method of Orientation

It is obvious that the powder to be oriented should consist of separate particles, each having only one crystallographic direction. The simplest way to achieve this condition is to grind a well-sintered material until it contains no aggregates comprising more than one crystal. This method, however, requires excessive milling, which inevitably will introduce a risk of contamination. A possible, though very highly academic, alternative method is to find suitable calcination conditions so as to produce single-crystal particles. This is one of the purposes of developing a suitable co-precipitation method.

Having found a suitable ferrite powder, the orientation can be achieved in a number of ways.

The first way takes advantage of the plate-like shape of ferrite crystals. By packing the powder in a steel tube, welding both ends of this tube and pressing it through a roll at high temperature, a preferred direction of magnetization perpendicular to the plane of rolling may be obtained (14). Similarly, in theory, an anisotropic magnet can be prepared merely by compressing the powder at high pressure.

The more efficient method of orienting the powder takes advantage of its magneto-crystalline anisotropy.

Neglecting all other terms but the first of Equation 1 (page 12), the anisotropic energy expression becomes:

$$E_k = K_1 \sin^2 \alpha \qquad \ldots \text{(Eq.16)}$$

The torque exerted on the particle will be

$$T = \frac{\partial E_k}{\partial \alpha} = K_1 \sin 2\alpha \qquad \ldots \text{(Eq.17)}$$

T will be maximum when $\alpha = 45°$.

From Equation 5, it can be shown that there is no value of H that will exert a maximum torque (equal to K_1 in magnitude) on all the particles simultaneously, since they have different α_o values. It is reasonable to assume however, that the most difficult particles to align physically are those whose c-axes happen to be perpendicular to the direction of H. For this reason, it may be profitable to exert a maximum torque on these particles, while other particles will experience a somewhat less torque. In this case, the external field required will be

$$H = (K_1/M_s)\sqrt{2} = 0.5\, H_a \sqrt{2} \qquad \ldots \text{(Eq.18)}$$

For $BaO.6{\cdot}0\,Fe_2O_3$, this value turns out to be about 11,000 Oe.

If the external field H is greater than the above value, the angle α will be greater than 45° and the torque will decrease. For $H = H_a$, α will be 90° and the torque will be zero.

A magnetic particle introduced into a magnetic field will turn itself into its most favourable direction from the magnetic point of view only if it can overcome the physical resistance that it encounters. To obtain maximum efficiency, then, it is necessary to minimize the tendency of one particle to impede the orientation of another. One way of doing this is to orient the powder in the form of slurry. The application of the orienting field in an intermittent way causes agitation of the particles in the slurry and further assists towards perfection of orientation.

Once the particles in the magnetic field are properly aligned, they must be stabilized. This can be accomplished by applying pressure to form a compact and then sintering it. During the sintering however, it must be borne in mind that grain growth should be avoided as far as possible if the coercive force is to be maintained. The change in the coercive force with grain size is more critical for oriented specimens than for isotropic specimens (10).

3. Degree of Orientation

Qualitatively, the degree of orientation of a certain ferrite magnet can be observed under a microscope from polished sections prepared from two slices that are cut perpendicular to each other (10).

A more quantitative measure of the orientation is given by the ratio of the residual magnetization perpendicular to its easy direction $M_{r\perp}$ to the residual magnetization along the easy direction $M_{r//}$ (14).

If it can be assumed that no magnetization processes other than domain rotation occur, then, for a completely-oriented specimen, $M_{r\perp} = 0$ and $M_{r//} = M_s$; also, for a completely random specimen, $M_{r\perp} = M_{r//} = 0.5\, M_s$.

Therefore $M_{r\perp}/M_{r//} = 0$ for a fully-oriented specimen

$= 1$ for a completely random specimen.

Alternatively, the degree of orientation of a specimen can be measured using an X-ray diffraction technique. If a completely-oriented specimen is placed in an X-ray diffractometer in such a way that the incident beam hits the basal plane, only (00ℓ) reflections will be observed. This result can be employed to express the degree of orientation.

Lotgering (15) has expressed the degree of orientation by the value of f, which is defined as:

$$f = \frac{(P-P_o)}{(1-P_o)} \qquad \ldots \text{(Eq.19)}$$

where $P = \dfrac{\Sigma I_{(00\ell)}}{\Sigma I_{(hk\ell)}}$ for an oriented specimen being examined

$P_o = \dfrac{\Sigma I_{(00\ell)}}{\Sigma I_{(hk\ell)}}$ for a completely random specimen

$I_{(hk\ell)}$ = intensity of the $(hk\ell)$ reflection.

f will have a value of zero for a completely random specimen and unity for a completely-oriented specimen.

The intensity reflected from a plane specimen can be expressed as

$$I_{(hk\ell)} \approx F^2_{(hk\ell)} \cdot m. \frac{1 + \cos^2\theta}{\sin^2\theta \cos\theta} \qquad \ldots \text{(Eq. 20)}$$

where m = multiplicity factor of the plane $(hk\ell)$,

F = structure factor,

θ = Bragg angle.

The angular factor of the above expression $f(\theta)$ is very sensitive to the value of θ at low angles, not sensitive at medium values of θ and becomes increasingly sensitive at high Bragg angles. For this reason, using intensity for computing P value, gives more weight to the low-angle reflections. Therefore, it may give a better representation if the following expression is used to compute P instead of the intensity.

$$P = \left(\frac{\sum \{F^2_{(00\ell)} \cdot m_{(00\ell)}\}}{\sum \{F^2_{(hk\ell)} \cdot m_{(hk\ell)}\}} \right)_{\text{observed}} \qquad \ldots \text{(Eq. 21)}$$

The X-ray diffraction method for expressing the degree of orientation has the advantage that it is independent of both ceramic conditions and magnetic measurement techniques. The limitation of the method is that it cannot be used to compare the degree of orientation of specimens of different compositions, since the atoms contributing to each reflection (and, presumably their parameters) will vary from one composition to another.

Gillam and Smethurst (16) modified Lotgering's expression by inserting a cosine $\Phi_{(hk\ell)}$ factor, where $\Phi_{(hk\ell)}$ is the angle between the $(hk\ell)$ plane and the (00ℓ) plane.

FACTORS AFFECTING MAGNETIC QUALITY

The properties of magnetic materials depend, among other things, on their chemical composition, fabrication and heat treatment. Some properties, such as saturation magnetization, vary very little with these factors. Other properties, such as coercive force, are very sensitive to changes in some of the above factors. These factors are, of course, interrelated and, therefore, it is difficult to describe one factor without mentioning the others. In order to simplify the discussion, these factors will be discussed separately.

1. Effect of Chemical Composition

The effects of chemical composition on both ceramic and magnetic properties of ferrite-type permanent magnets can be classified into two parts: (a) the effect of the stoichiometric ratio of Fe_2O_3/MO and (b) the effect of impurities.

(a) The Effect of the Stoichiometric Ratio of Fe_2O_3/MO

Kojima et al. (17-22) prepared the Ba, Sr and Pb ferrites, having the Fe_2O_3/MO ratio from 4.4 to 6.6, by the dry method. They calcined the powders at 900°C for two hours and then sintered the specimens at from 1100 to 1200°C for 15 minutes. The forming pressure was 6 ton/cm^2. The saturation magnetization, remanent induction and intrinsic coercive force were measured. The maximum magnetic field applied was 10,000 oersted. The saturation magnetization for $BaO.6{\cdot}0\,Fe_2O_3$ sintered at 1200°C was reported to be about 3300 gauss. This is much lower than the value reported by Stuijts et al. (14), which is 4775 gauss. This low value may be partly due to low density, but also may be a result of the low external field applied during measurement. It is difficult to believe that 10,000 oersted would be a high enough field to saturate an isotropic specimen. However, these results illustrate the general trend of the magnetic properties with varying composition just as well as if they had measured the specimens with a much higher field, since the most important factor is the relative change (23).

For barium ferrite, both the saturation and the remanent magnetization increased slowly as the ratio was increased from $n = 4.4$ to about 6. They then suddenly decreased at $n \approx 6$. There was no appreciable change in the coercive force with increasing n, except for the specimen sintered at 1150°C. In this case, the coercive force increased sharply at $n \approx 6$. This sudden change in the magnetic properties at $n \approx 6$ is in agreement with the sudden change in the shrinkage at this composition observed by Stuijts (24). He investigated the shrinkage of barium ferrite with values of n from 5.6 to 6.0, sintered at 1050 to 1300°C for two hours in air. The higher the sintering temperature, the higher was the drop in percentage shrinkage at $n \approx 6$.

In the case of strontium hexaferrite, the behaviour was similar to that of the barium compound, except that there was a little peak of saturation magnetization at $n = 5$.

For lead hexaferrite, however, the behaviour was different. The maximum remanent and saturation magnetizations occurred at $n = 4.5$. Kojima et al. (18) predicted the existence of a ferrimagnetic compound having the formula $MO.4{\cdot}0\,Fe_2O_3$ for both strontium and lead. This prediction was supported by Mountvala and Ravitz (5), who suggested that the lead compound has a homogeneity range from $n = 5.0$ to 6.0, and explained the homogeneity by a crystallographic argument. He proposed an absence of up to three oxygen ions in the Ba-plane and of the two iron atoms associated with them. A complete absence of this trigonal bipyramid will result in the composition $PbO.5{\cdot}0\,Fe_2O_3$. Since these Fe^{III} ions are in the minority sublattice, the net moment of the compound will increase by an amount equivalent to that due to the presence of a maximum of two Fe ions. This explains the maximum of magnetization occurring at about this composition(18).

(b) The Effect of Impurities

Although it is very difficult to predict theoretically how the presence of a certain foreign element will affect a given ceramic body, these elements must fall into one or other of the following categories.

(i) Those which do not enter the lattice

These impurities will precipitate on the grain boundaries and will probably affect the ceramic properties of the specimen, rather than the intrinsic magnetic properties.

(ii) Those elements that will enter the lattice (substitution)

Cation substitition in barium ferrite can be divided into two types, according to whether or not charge compensation is required. Charge compensation is not required when direct isovalent substitution is made, such as when large divalent ions, notably Pb^{+2} and Sr^{+2} partly or entirely replace Ba^{+2}, or when Al^{+3}, Ga^{+3} or Cr^{+3} are introduced directly as substituents for Fe^{+3}. But, if divalent ions are used to replace Fe^{+3}, charge compensation is required to maintain electrical neutrality.

Another method of grouping the substituents is according to whether they replace the Ba^{+2} ions or whether they replace the Fe^{+3} ions. The latter type can enter the lattice in tetrahedral or octahedral interstices or at random in the spinel block.

In theory, one should be able to alter the magnetic properties of barium ferrite intrinsically by substituting for Fe^{+3} with a substituent which will preferentially enter the lattice at certain locations in the spinel block. A substituent with fewer unpaired electrons than Fe^{3+} in the minority sublattice should increase the saturation magnetization, and vice versa. However, in practice, other complications must be considered. Mones and Banks (29) determined the fate of Al, Ga and Zn when substituted in barium ferrite. They determined whether the substituents occupied preferential locations or were randomly distributed in the spinel block. They compared the calculated value of β to its observed value, where:

$$\beta = \frac{\text{magnetization of substituted barium ferrite}}{\text{magnetization of pure barium ferrite}} \quad \ldots (\text{Eq.22})$$

They found that, for Ga^{+3} at below 0.3 gram atoms of Ga per mole of ferrite, the ions will occupy the tetrahedral sites, and above 0.3, will be randomly distributed. This complication is worsened by the possibility of the formation of other types of hexagonal ferrites such as the Y and W compounds which have a planar magnetization direction.

The following is a summary of the effects of various substituents on the magnetic properties of ferrites as reported in the literature.

Effects of Bi_2O_3 (17, 18)

1. The effects of Bi_2O_3 could not be recognized in Pb ferrite.
2. The values of $4\pi M_s$ and $4\pi M_r$ for Ba ferrite are always increased by the addition of Bi_2O_3. For Sr ferrite, they increase only for $Fe_2O_3/SrO>6$.
3. The value of iH_c for Ba ferrite is increased by 40 to 50% by the addition of Bi_2O_3, while the value of iH_c for Sr ferrite decreases with this addition.
4. The effects of Bi_2O_3 on (Sr, Ca) ferrite, sintered at lower temperatures, are similar to the effects on Ba ferrite, except that the value of iH_c is decreased remarkably in the range of $CaO<1.5\%$ and the diminution was regained at about $CaO = 3\%$.
5. The above effects of Bi_2O_3 on the magnetic properties are not intrinsic but are due to the acceleration of the sintering process.

Effects of TiO_2 (19)

1. The magnetic properties deteriorate with the addition of TiO_2 except in the case of $Fe_2O_3/MO = 4$. For Ba ferrite with this ratio, the values of $4\pi M_s$ and $4\pi M_r$ become maxima at $TiO_2 = 5\%$ and iH_c is a maximum at $TiO_2 = 7\%$. For both Sr and Pb ferrites, these maxima occur at $TiO_2 = 1$ to 3%.
2. Mones and Banks (23) proposed that the Ti^{+4} ions enter the lattice and occupy the octahedral interstices of the spinel block. The same behaviour occurs for Mg^{+2} and Cr^{+3}.

Effects of Al_2O_3 (20)

1. Al_2O_3 decreases the values of both $4\pi M_s$ and $4\pi M_r$ for Ba, Sr and Pb ferrites, except for Ba ferrite with Fe_2O_3/BaO ratio $n<4.5$.
2. The value of n for which $4\pi M_s$ and $4\pi M_r$ are maxima for Ba ferrite is shifted by the addition of Al_2O_3. No apparent shift occurs in either Sr or Pb ferrites.
3. The value of iH_c is increased by the addition of Al_2O_3.
4. Mones and Banks (23) proposed that the aluminum ions occupy octahedral interstices in the spinel block.

Effects of SiO_2, B_2O_3, GeO_2, Cr_2O_3, CdO, SnO, CoO, CuO and V_2O_5 (22)

The effects of these additives on the magnetic properties of Ba ferrite might be due to their increasing the apparent density and to their inhibiting of the grain growth, rather than due to the formation of a new ferromagnetic phase.

1. CdO, SnO, CoO, and CuO are not effective as additives in improving the values of $4\pi M_r$ or iH_c in the Ba and Sr ferrites.
2. SiO_2, B_2O_3, GeO_2 and Cr_2O_3 are fairly effective for both systems.
3. V_2O_5 is injurious.

Sulphate-modified Sr ferrite

Of all the additives that have been reported, a small quantity of sulphate, particularly in Sr ferrite seems to be the most effective (2, 25). The effectiveness of the sulphate additive depends on the quantity, the step in the manufacturing process at which the addition is made, and the form in which the sulphate is added.

The optimum quantity of sulphate additive in Sr hexaferrite has been reported to be between 0.2 and 1.0% metal sulphate. This amount of sulphate caused an increase in the $(BH)_{max}$ from about 3.4×10^6 gauss-oersted to about 4.0×10^6 gauss-oersted. The additive in the form of $SrSO_4$ was reported to be more effective than in the form of $CaSO_4$ or $BaSO_4$. In order to optimize the sulphate effect, the addition process must be so chosen that the sulphate is able to dissolve in the matrix. Cochardt (25) recommended that the sulphate be added to the raw materials and that the particles be small in the initial mix. Another requirement is that the calcination conditions should be such that the sulphate does not decompose completely.

The sulphate additive was reported to be particularly beneficial when in combination with other additives such as Al_2O_3 and SiO_2. This effect was shown in strontium hexaferrite prepared by the "celestite process", using the mineral celestite as one of the raw materials (2). A typical analysis of celestite is 92% $SrSO_4$, 4.5% $CaSO_4$, 1.5% $BaSO_4$, 1.5% SiO_2 and 0.5% Al_2O_3. Energy products, $(BH)_{max}$, as high as 4.8×10^6 gauss-oersted have been achieved with this process.

Ba-Sr-Pb-ferrite system

The three binary sub-systems of this ternary system have been investigated by Borovik and his co-workers (26,27, 28). They investigated the magnetic properties of both isotropic and anisotropic specimens of $(Ba_{1-x}Sr_x)O.6\cdot0Fe_2O_3$ and isotropic specimens of $Ba_{1-x}Pb_x)O.6\cdot0Fe_2O_3$ and $(Sr_{1-x}Pb_x)O.6\cdot0Fe_2O_3$ for $0 \geq x \geq 1$.

The powders were prepared from Ba, Sr and Pb carbonates and iron oxide by the dry method, calcined for five hours at 1100°C for those without Pb, and at 900°C for those containing lead.

For the isotropic $(Ba_{1-x}Sr_x)O.6\cdot0Fe_2O_3$ specimens (26), the forming pressure was 17 ton/cm^2; they were sintered at 1200 to 1300°C. Their results are reproduced in Figure 13. They found that specimens with x = 0.25 sintered at 1230°C give the best properties. The energy product of these specimens was 1.45×10^6 gauss-oersted. The highest coercive force was found to be 4200 oersted for x = 1 (i.e. pure Sr ferrite). Hutny (29) disagrees with this finding. He has stated that the presence of strontium does not improve the sintering behaviour. The density of his specimens containing strontium was less than that of pure barium ferrite. He maintains that the larger remanent magnetization and energy product of the ferrites containing strontium are due to a certain amount of anisotropy caused by the extremely high forming pressure (17 ton/cm^2).

In a later paper (27), they reported that this optimum composition is the same for anisotropic specimens. They reported the highest $(BH)_{max} = 2.9 \times 10^6$ gauss-oersted for a sample having x = 0.25 that was sintered at 1230°C. They claimed that this value was reproducible. Their results are shown in Figure 14.

For $(Ba_{1-x}Pb_x)$ and $(Sr_{1-x}Pb_x)$ ferrites, they investigated only isotropic specimens (28). Their results, which are reproduced in Figure 15, indicated that the addition of lead will lower both the intrinsic coercive force, iH_c, and remanent magnetization, B_r. It must be noted here that, for high values of x, Br and iH_c decreased as the sintering temperature and x were increased. In view of the lack of analytical evidence in this paper, there is some suspicion that the decrease of these values may have been due to the volatilization of lead. This behaviour has been observed in this laboratory on heating lead ferrite at 1200°C for 12 hours in air.

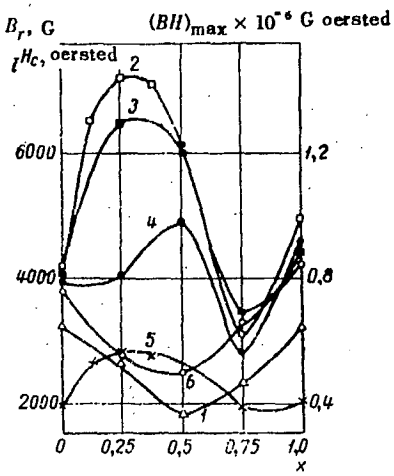

Curves showing the composition dependence of erties of mixed ferrites $Ba_{1-x}Sr_xO \cdot 6Fe_2O_3$ at various different sintering temperatures:

$(BH)_{max}$ at: 1 -- 1200;
2 -- 1230;
3 -- 1260;
4 -- 1300°C;
5 -- B_r at 1230°C;
6 -- $_jH_c$ at 1230°C.

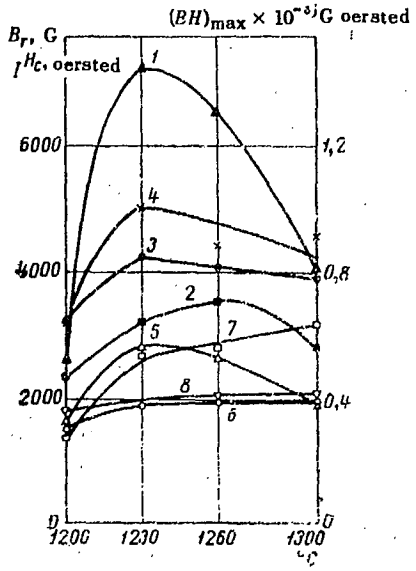

FIG. 2. Dependence of properties of mixed ferrites on sintering temperature for various different compositions:

$(BH)_{max}$ for 1 — $Ba_{0.75}Sr_{0.25}O \times 6Fe_2O_3$, 2 — $Ba_{0.25}Sr_{0.75}O \cdot 6Fe_2O_3$, 3 — $BaO \cdot 6Fe_2O_3$, 4 — $SrO \cdot 6Fe_2O_3$; B_r for: 5 — $Ba_{0.75}Sr_{0.25}O \cdot 6Fe_2O_3$, 6 — $Ba_{0.25}Sr_{0.75}O \cdot 6Fe_2O_3$, 7 — $Ba_{0.5}Sr_{0.5}O \cdot 6Fe_2O_3$, 8 — $BaO \times 6Fe_2O_3$.

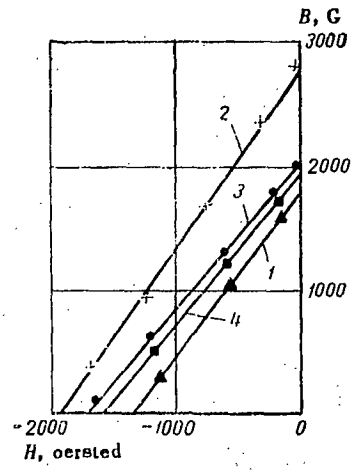

Demagnetization curves for different ferrites (sintering temperature 1230°C):

1 — $Ba_{0.25}Sr_{0.75}O \cdot 6Fe_2O_3$; 2 — $Ba_{0.75}Sr_{0.25}O \cdot 6Fe_2O_3$; 3 — $SrO \cdot 6Fe_2O_3$; 4 — $BaO \cdot 6Fe_2O_3$.

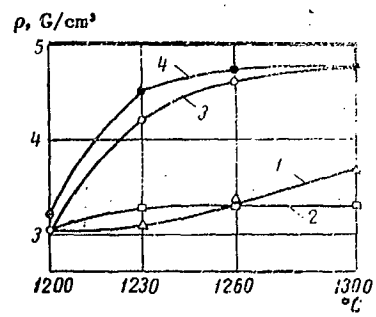

FIG. 4. Density ρ as function of sintering temperature for different ferrites:

1 — $SrO \cdot 6Fe_2O_3$. 2 — $Ba_{0.25}Sr_{0.75}O \times 6Fe_2O_3$; 3 — $Ba_{0.5}Sr_{0.5}O \cdot 6Fe_2O_3$; 4 — $Ba_{0.75}Sr_{0.25}O \cdot 6Fe_2O_3$.

Figure 13. Magnetic Properties of Isotropic $(Ba_{1-x}Sr_x)O.6 \cdot 0Fe_2O_3$ (Reproduced from Reference 26).

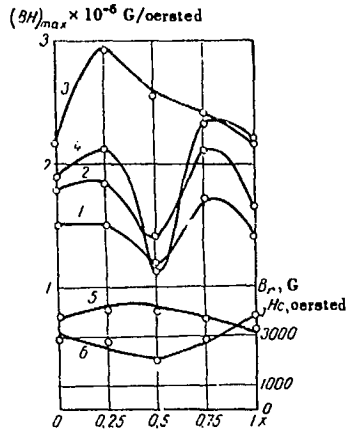

FIG. 1. Composition dependence curves for the magnetic properties of anisotropic mixed ferrites $Ba_{1-x}Sr_x$ 0.6 Fe_2O_3 at various different sintering temperatures:
1 – $(BH)_{max}$, T = 1100°C;
2 – $(BH)_{max}$, T = 1200°C;
3 – $(BH)_{max}$ T = 1230°C;
4 – $(BH)_{max}$, T = 1260°C;
5 – B_r, T = 1230°C;
6 – $_jHc$, T = 1230°C.

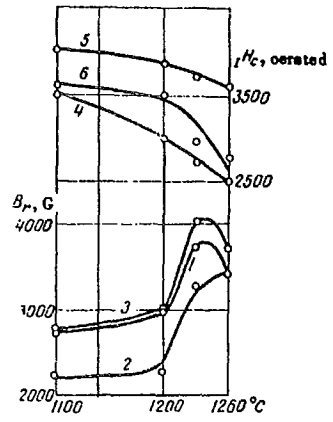

FIG. 3. Curves showing the dependence of B_r the residual magnetization and $_jHc$ the coercive force of anisotropic mixed ferrites on sintering temperature:
1 – B_r curve Ba 0.6 Fe_2O_3;
2 – B_r curve Sr 0.6 Fe_2O_3;
3 – B_r curve $Ba_{0.75}$ $Sr_{0.25}$ 0.6 Fe_2O_3.
4 – $_jHc$ curve Ba 0.6 Fe_2O_3;
5 – $_jHc$ curve Sr 0.6 Fe_2O_3;
6 – $_jHc$ curve $Ba_{0.75}Sr_{0.25}$ 0.6 Fe_2O_3.

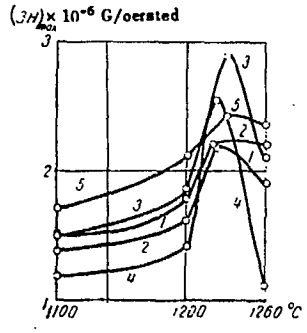

FIG. 2. Curves showing the dependence of the maximum magnetic energy for systems of anisotropic mixed ferrites Ba_{1-x} Sr_x 0.6 Fe_2O_3 on sintering temperature:
1 – Ba 0.6 Fe_2O_3;
2 – Sr 0.6 Fe_2O_3;
3 – $Ba_{0.75}Sr_{0.25}$ 0.6 Fe_2O_3;
4 – $Ba_{0.5}$ $Sr_{0.5}$ 0.6 Fe_2O_3;
5 – $Ba_{0.25}$ $Sr_{0.75}$ 0.6 Fe_2O_3.

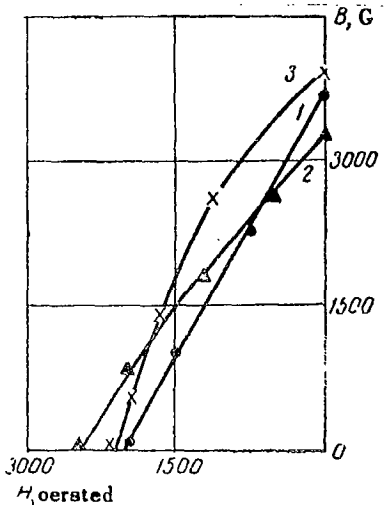

FIG. 4. Demagnetization curves for anisotropic ferrites of different composition. Sintering temperature 1230°C:
1 – curve Ba 0.6 Fe_2O_3;
2 – curve Sr 0.6 Fe_2O_3;
3 – curve $Ba_{0.75}Sr_{0.25}$ 0.6 Fe_2O_3.

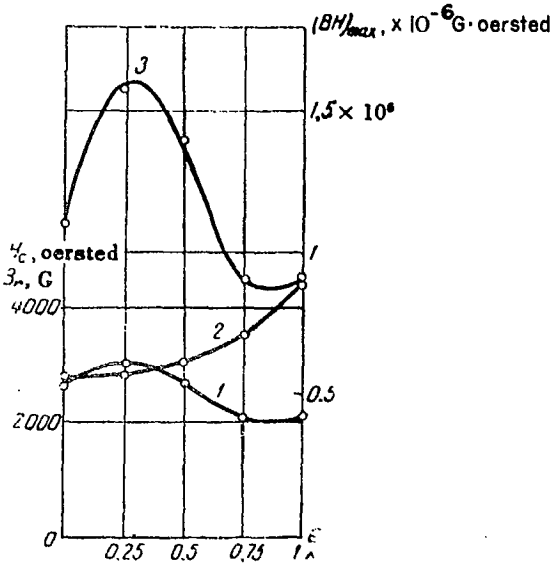

FIG. 5. Composition dependence curves for the properties of isotropic specimens of mixed ferrites $Ba_{1-x}Sr_x$0.6 Fe_2O_3 for sintering temperature 1230°C:
1 – B_r; 2 – $_jHc$;
3 – $(BH)_{max}$.

Figure 14. Magnetic Properties of Anisotropic $(Ba_{1-x}Sr_x)O.6\cdot 0Fe_2O_3$ (Reproduced from Reference 27).

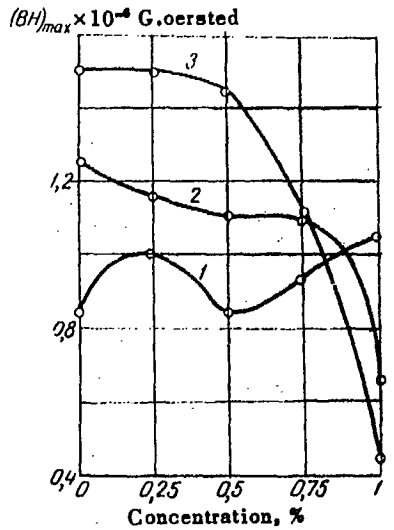

FIG. 1. $(BH)_{max}$ versus composition for a system of isotropic mixed ferrites $Ba_{1-x}Pb_x O \cdot 6Fe_2O_3$ at sintering temperatures:
1 – 1100°; 2 – 1200°; 3 – 1230°C.

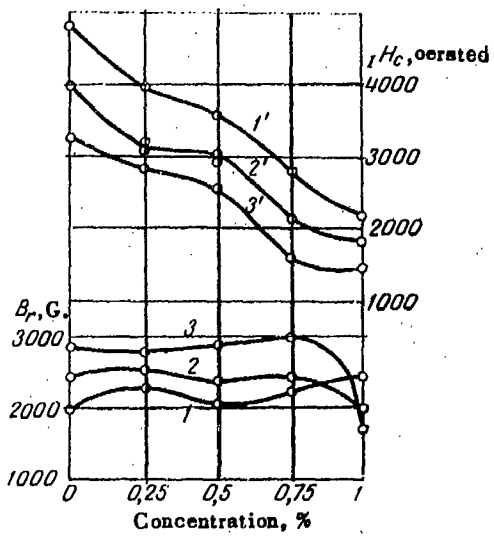

FIG. 2. B_r (1-3) and $_IH_c$ (1′-3′) versus composition isotropic mixed ferrites $Ba_{1-x}Pb_x O \cdot 6Fe_2O_3$ at sintering temperatures:
1 – 1′ – 1100°; 2 – 2′ – 1200°; 3 – 3′ – 1230°C.

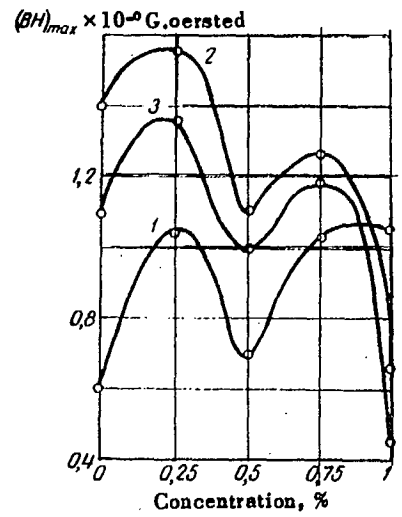

FIG. 3. $(BH)_{max}$ versus composition for a system of isotropic mixed ferrites $Sr_{1-x}Pb_x O \cdot 6Fe_2O_3$ at sintering temperatures:
1 – 1100°; 2 – 1200°; 3 – 1230°C.

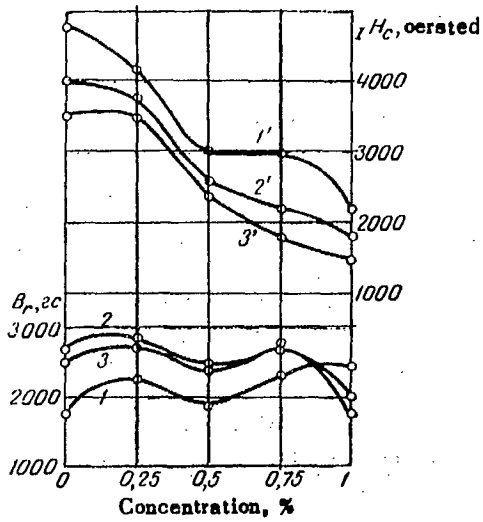

FIG. 4. B_r (1-3) and $_IH_c$ (1′-3′) versus composition f isotropic mixed ferrites $Sr_{1-x}Pb_x O \cdot 6Fe_2O_3$ at sintering temperatures:
2 – 2′ – 1100°; 1 – 1′ – 1200°; 3 – 3′ – 1230°C.

Figure 15. Magnetic Properties of Isotropic $(Ba_{1-x}Pb_x)O.6 \cdot 0Fe_2O_3$ and $(Sr_{1-x}Pb_x)O.6 \cdot 0Fe_2O_3$ (Reproduced from Reference 28).

2. Effect of Fabrication

As has been discussed previously, the most important fabrication variable, from the point of view of the magnetic properties of the finished ceramic ferrite magnet, is the degree of crystallographic orientation. Another factor that might affect the magnetic properties is the forming pressure. There has been no systematic study published about the effect of this variable, but the use of forming pressures as low as the roller pressure employed in the "Ferriroll Process" (30), and as high as 17 ton / cm^2 (26) have been reported.

3. Effect of Heat Treatment

The heat treatment of permanent-magnet-type ferrites is one of the most important factors in the preparation. It may be as important as, and very closely related to, their composition and the physical properties of the raw materials. It has been stated previously that a number of additives affect the magnetic properties of the specimen, not intrinsically, but by affecting its heat-treatment behaviour.

The heat treatment of ferrite ceramics usually consists of two steps.

(a). Pre-sintering or Calcination

In this stage of heat treatment, the raw materials are reacted to form the ferrite compound $MO.nFe_2O_3$, and also the ferrite crystals are allowed to develop and grow to a sufficient size. The limit of the development of the crystals is very important, depending on the further processes that will be employed. If extensive comminution, such as by ball-milling, is anticipated, the crystals should be allowed to grow sufficiently large to ensure that the ground powder will consist of single-crystal particles. On the other hand, if extensive grinding is to be avoided, crystal growth should be stopped at below 1 μ, the critical diameter. This control, however, is very difficult to attain since the reaction itself (in the case of barium and strontium ferrites) occurs at such high temperatures that simultaneous sintering and grain growth is difficult to avoid if the reaction is to be completed. However, Lotgering (15) has prepared oriented larger-molecule hexagonal ferrites by reacting the oriented $MO.6{\cdot}0\,Fe_2O_3$-type ferrites with the other components in the cubic form. If the grain growth of the M compound takes place by a mechanism similar to that in Lotgering's reaction, then it may be possible to pre-sinter the ferrite to near-completion of its reaction, and then, during sintering of the oriented sample, the residue of the unreacted materials will be absorbed by the oriented ferrite crystals. The condition that may be required here is, among other things, that the unreacted materials should be finer than the ferrite particles.

(b) Sintering

The second step of the heat treatment is the sintering of the fabricated specimens. The purpose of this operation is to densify the specimen and also, possibly, to complete the reaction and to improve the orientation. There are two important factors that must be controlled in this stage of heat treatment. The first is the grain growth and the second is the possibility of losing volatile elements such as lead and oxygen from the ceramic body.

Stuijts et al. (14) investigated the effect of the sintering temperature on various magnetic properties. Their results are reproduced in Figure 16. Van Hook (31) investigated the thermal stability of barium ferrite. He concluded that barium hexaferrite is stoichiometric in oxygen content and in cation ratio within the limits of detection, having the formula $Ba_{(1 \pm 0.04)} Fe_{12} O_{(19 \pm 0.03)}$ from room temperature up to 1450°C at 1 atm oxygen pressure. His phase diagrams reproduced in Figures 17A and 17B.

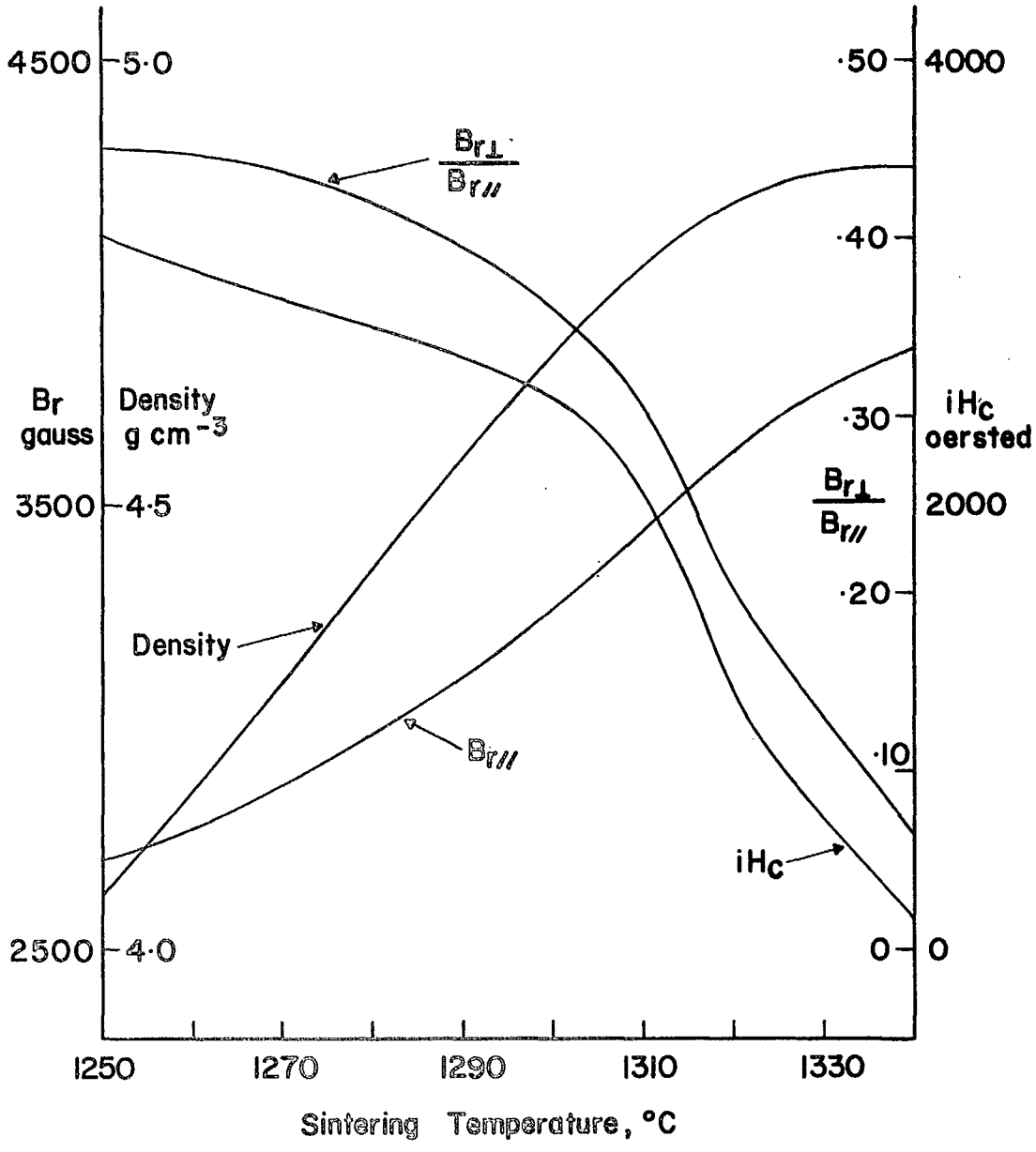

Figure 16. Variation of Density, B_r and iH_c with the Sintering Temperature of Ferroxdure (oriented), (Reproduced from Reference 14).

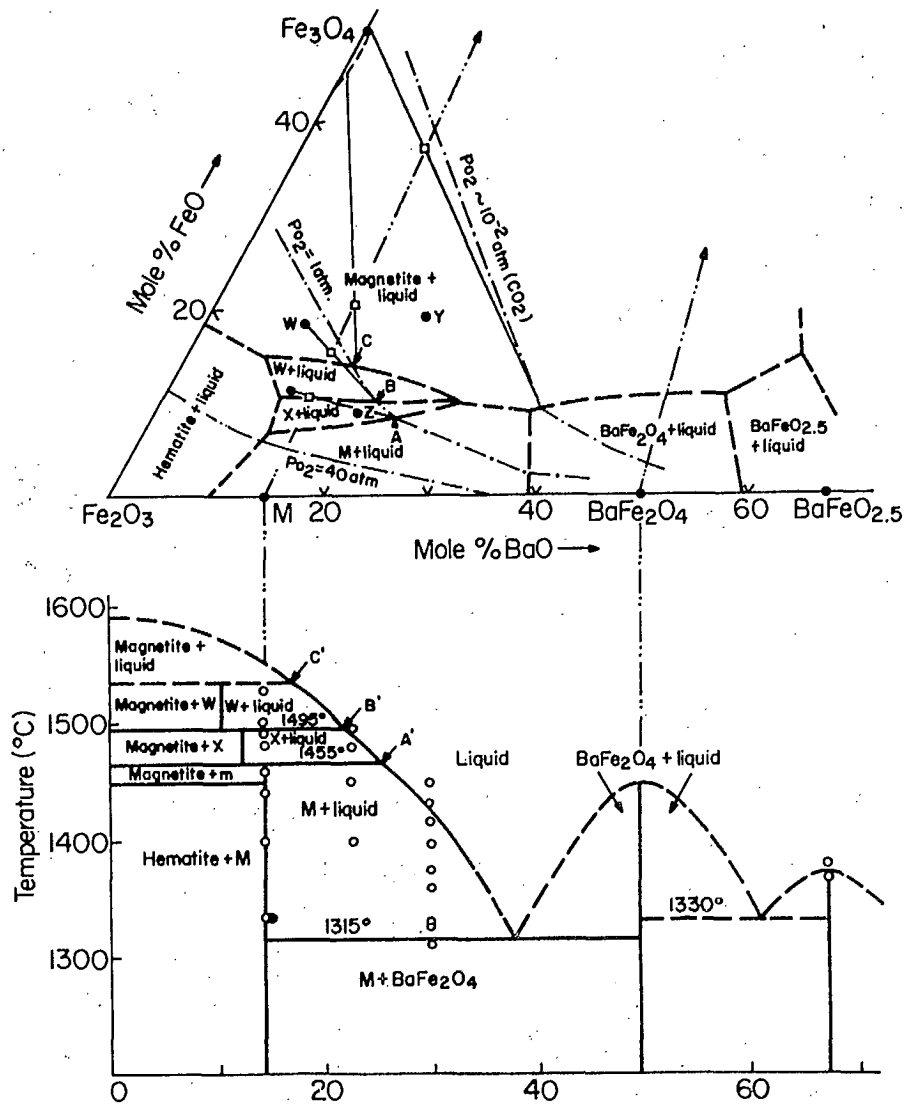

Fig. 17A The ternary system Fe_2O_3–FeO–BaO and the isobaric projection at 1 atm oxygen pressure. Three isobars (dash-dot lines) are shown in the ternary diagram, one of which (1 atm) is also represented in projection. Dash–double-dot lines are oxygen reaction lines. Square symbols indicate composition of coexisting liquid and crystalline phases joined by tie lines. Heavy dashed lines indicate inferred phase relations.

(Reproduced from Reference 31).

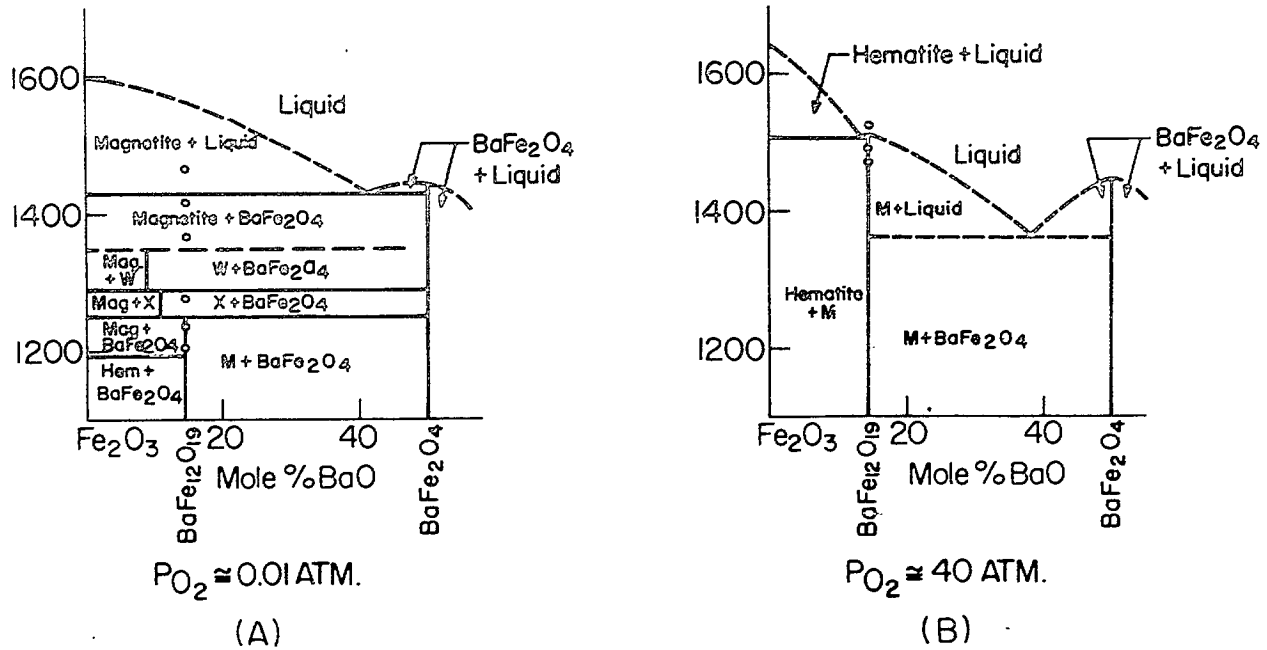

FIG 17B Projections of two oxygen isobaric sections in the system Fe_2O_3–FeO–BaO.

(Reproduced from Reference 31).

METHOD OF PREPARATION

Two factors must be considered in choosing the method of preparation in order to obtain a good ferrite body.

1. Chemical factors: these include the exactness of the composition in terms of the major elements, i.e., the iron, barium, strontium and lead, the valency of the iron and the type and required amount of additive to achieve certain desired properties. This composition must be homogeneous down to the individual grains.
2. Ceramic factors: these include grain size, density, porosity, crystal orientation, mechanical strength, etc.

Most of the literature available on the method of preparation of ferrites is concerned with the preparation of soft or spinel-type ferrites. It must be borne in mind, however, that there are important differences between the method of preparation of soft and hard or hexagonal-type ferrites, from both the chemical and structural points of view. Chemically, the metal components of soft ferrites, such as cobalt, nickel and iron, are very similar. In some cases, it is possible to form a solid solution of a common salt, for example, Ni - Fe oxalates. In other cases, they may form crystals with very close physical similarities, thus permitting good co-precipitation.

In the case of permanent-magnet-type ferrites, there are no common salts of barium, strontium and/or lead and Fe^{+3} that will, co-precipitate quantitatively. It is possible to precipitate iron and barium together as oxalates if the iron can be kept in the ferrous state. But the difficulty in this case is that there are no common soluble ferrous salts that are stable enough, since ferrous ammonium sulphate is out of the question on the account of the insolubility of barium sulphate. The required ratio of barium, strontium and/or lead to iron of 1:6·0 eliminates the possibility of using a double oxalate.

Structurally, in the spinel-type ferrites, both metals occupy interstitial sites within the oxygen close-packed framework. The ionic radii of all these metals are of the same order of magnitude. On the other hand, the barium, strontium and/or lead in the hexagonal ferrites replace oxygen in the R-block. For these reasons, the methods that are used for the preparation of spinel-type ferrites are not necessarily applicable to hard-ferrite preparation.

Schematically, all the methods of preparation can be illustrated in Figure 18. The middle column shows the processes in various stages, the left-hand column described the process-control variables and the right-hand column indicates the quality control of intermediate products at various stages.

The variations between the methods generally occur in the method of mixing the raw materials. The aim of this operation is first to mix the materials into a desired composition. This composition has to be homogeneous down to the smallest possible fraction. The second aim is to provide as large a contact area as possible between one raw material and another, thus accelerating the rate of reaction and lowering the calcination temperature.

It has been mentioned in a previous section of this report that, for the purpose of orienting the crystals, the particles must be magnetic; hence, they must be well-reacted since the raw materials are not magnetic. The powder should consist of particles that are either single-crystal or, if polycrystalline, the individual crystallites must have their c-axes all oriented in the same direction. Composite particles, in which sintering has resulted in the presence of crystallites with varying orientations, must be avoided. The powder must be kept as free as possible from undesirable (i.e., unknown) impurities; thus, excessive grinding is undesirable since it promotes contamination.

There are two main reactions occurring during calcination that can be simplified as follows:

$$(Ba,Sr,Pb)CO_3 + 6{\cdot}0\,Fe_2O_3 \longrightarrow (Ba,Sr,Pb)O.6{\cdot}0\,Fe_2O_3 \quad (1)$$

$$n(Fe_2O_3)_{\text{small particle}} \longrightarrow (Fe_2O_3)_{\text{large particle}} \quad \text{(sintering)} \quad (2)$$

Reaction (1), of course, consists of a number of stages with several intermediate products depending on the raw materials and the degree of mixing. Hence, the rate of the total reaction (1) depends also on these factors. The ideal situation would be that reaction (1) should be completed before reaction (2) begins. In practice, one tries to minimize reaction (2). To achieve this, the barium, strontium and/or lead component must be of comparable reactivity with the iron oxide.

The classical method of mixing the raw materials is by ball-milling. This type of milling will serve both for mixing and also for size-reduction. The drawback of this method is the inevitable introduction of impurities.

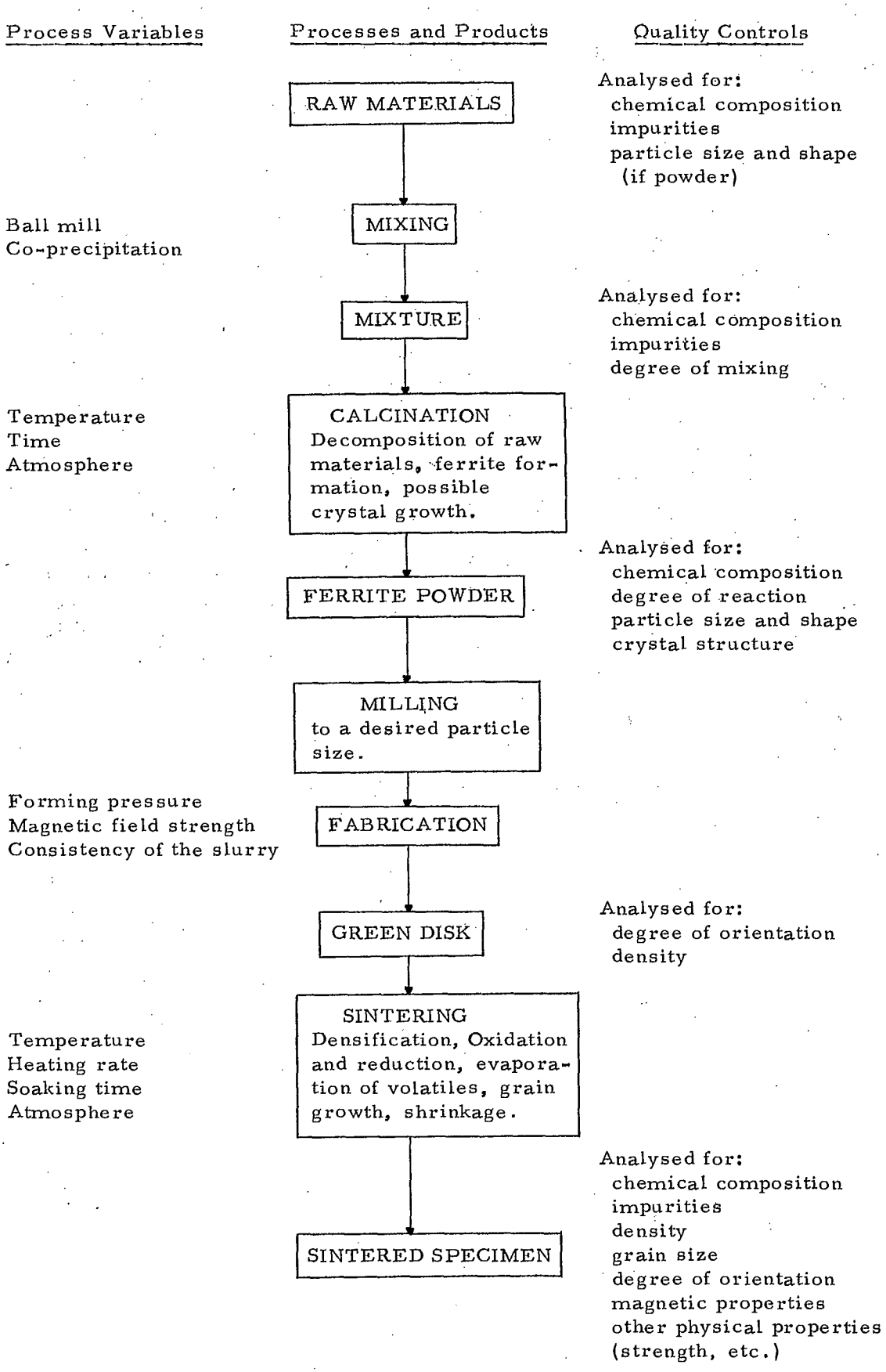

Figure 18. Schematic Diagram of Ferrite Manufacturing Processes.

The more elaborate method is by chemical co-precipitation. This method has been proven to be useful for some ceramic materials. The ideal case of co-precipitation occurs when the raw materials form a compound (usually a double salt) which, upon heating, will decompose into an active state of the metal components with the correct ratio, ready to react into the final product. This case occurs in the preparation of barium titanate via barium titanyl oxalate (32). In this case, the raw materials can be mixed in a convenient solution. Since a definite double salt is formed, the danger of segregation during the co-precipitation process is eliminated.

Unfortunately, there are no double oxalates or known similar compounds that give this metal ratio of 1:6·0; the only double oxalate known between these metals are barium and strontium trisoxalatoferrates^{III} with (barium, strontium) to iron ratio of 1:1 (33).

The next best way is to co-precipitate barium, strontium and/or lead and iron as different compounds whose particles have similar physical sizes and properties so that they will settle at the same rate.

The third possibility is by semi-co-precipitation. This method is based on the coating of an iron oxide powder with barium, strontium and/or lead salts. The iron oxide is mixed in a slurry with a convenient soluble barium salt solution. The pH is then adjusted and the barium is precipitated by a suitable precipitant such as carbon dioxide or ammonium oxalate. The advantage of this method is that the precipitate is easily filtered and more compact than that obtained by the full co-precipitation method. The drawbacks of this method are, of course, that the mixing of the raw materials is less intimate and that the reactivity of freshly-precipitated iron oxide is lost.

Another method that is possibly applicable is to mix the barium and iron salts in a suitable organic solvent. The mixed solution is then burned in an oxygen-rich flame. This process has been reported by Wenckus and Leavitt (34) for the preparation of soft ferrites. Exact quantitative control is difficult in this technique.

In the programme of work conducted in these laboratories, the various co-precipitation and semi-co-precipitation techniques have been employed.

ACKNOWLEDGEMENTS

This investigation was conducted under the direction of Dr. N. F. H. Bright, Head, Physical Chemistry Section, and Mr. I. F. Wright, co-ordinator of the Mines Branch Electronic Ceramics Programme, and was supported by the Defence Research Board of Canada under E.C.R.D.C. Project C-73.

The authors are indebted to Dr. A. H. Webster for his valuable discussion throughout the writing of this report.

The above-mentioned personnel, with the exception of Mr. I. F. Wright (Mineral Processing Division) are all members of the staff of the Mineral Sciences Division, Mines Branch.

REFERENCES

1. T. Takei, Kikai Denki, 2 [67], 379, 540 (1937) cited by (2).

2. A. Cochardt, "Recent Ferrite Magnet Developments", J. Appl. Phys., 37 [3], 1112-15 (1966).

3. N. F. H. Bright, A. H. Webster and I. F. Wright, "A Proposal for a Research Programme on Ferrites in the Mineral Sciences Division of the Mines Branch", Mineral Sciences Division Internal Report MS 65-98 (June 16, 1965).

4. Y. Goto and T. Takada, "Phase Diagram of the System BaO-Fe_2O_3", J. Am. Ceram. Soc., 43 [3], 150-53 (1960).

5. A. J. Mountvala and S. F. Ravitz, "Phase Relations and Structures in the System PbO Fe_2O_3", J. Am. Ceram. Soc., 45 [6], 286-88 (1962).

6. V. Adelskold, Arkiv Kemi, Min., Geol., 12A [29], 1-9 (1938) cited by (10).

7. Wyckoff, "Crystal Structure", Vol. III, Chapter XId. Intersciences Publisher Inc., New York (1960).

8. "International Tables for Crystallography", Vol. I, Published by the Kynoch Press, Birmingham, England. 304 (1952).

9. A. L. Stuijts, unpublished, cited by (10).

10. J. Smit and H. P. J. Wijn, "Ferrites", Published by John Wiley and Sons, New York (1959), various pages.

11. W. H. von Auloch, "Handbook of Microwave Ferrite Materials", Published by Academic Press, New York, (1965) pp. 462-84.

12. H. B. Casimir et al., "Report sur Quelques Recherches dans le Domaine du Magnétisme aux Laboratoires Philips", J. Phys. Radium, 20, 3069 (1957).

13. R. M. Bozorth, "Ferromagnetism", Published by D. Van Nostrand Company, Inc., Toronto (1951), various pages.

14. A. L. Stuijts, G. W. Rathenau and G. H. Weber, "Ferroxdure II and III, Anisotropic Permanent Magnet Materials", Philips Tech. Rev., 16 [5-6], 141-47 (1954).

15. F. K. Lotgering, "Topotactical Reactions with Ferrimagnetic Oxides having Hexagonal Crystal Structures: I", J. Inorg. Nucl. Chem., 9, 113-23 (1959).

16. E. Gillam and E. Smethurst, "The Orientation Texture and Magnetic Properties of Polycrystalline Barium Ferrite", Proc. Brit. Ceram. Soc., 2, 129-37 (1964).

17. T. Okamura, H. Kojima and S. Watabane, "Studies on the Oxide Magnets: I. Effect of Bi_2O_3 on Barium Ferrite", Sci. Rep. RITU, A7, 411-17 (1955).

18. T. Okamura, H. Kojima and S. Watabane, "Studies on the Oxide Magnets: II. Effect of Bi_2O_3 on Strontium and Lead Ferrites", Sci. Rep. RITU, A7, 418-24 (1955).

19. H. Kojima, "Studies on the Oxide Magnets: III. Effect of TiO_2", Sci. Rep. RITU, A7, 502-6 (1955).

20. H. Kojima, "Studies on the Oxide Magnets: IV. Effect of Al_2O_3", Sci. Rep. RITU, A7, 507-14 (1955).

21. H. Kojima, "Effect of Additionals on the Magnetic Properties of $PbO-Fe_2O_3$ System", Sci. Rep. RITU, A8, 540-46 (1956).

22. H. Kojima, "Effect of some Additionals for the Magnetic Properties of Ba and Sr Oxide Magnets", Sci. Rep. RITU, A10, 175-82 (1958).

23. A. H. Mones and E. Banks, "Cation Substitution in $BaFe_{12}O_{19}$", J. Phys. Chem. Solids, 4, 217-222 (1958).

24. A. L. Stuijts, "Sintering of Ceramic Permanent Magnetic Material", Trans. Brit. Ceram. Soc., 35, 57-74 (1956).

25. A. Cochardt, "Effects of Sulfates on the Properties of Strontium Ferrite Magnets", J. Appl. Phys., 38, [4], 1904-1908 (1967).

26. Ye. S. Borovik and N. E. Usikova, "Properties of Mixed Barium and Strontium Ferrites", Fiz. Metal. Metalloved., 13, [3], 470-73 (1962). (English translation).

27. Ye. S. Borovik and N. G. Yakovleva, "Influence of Texture on the Magnetic Properties of Mixed Barium and Strontium Ferrites", Fiz. Metal. Metalloved., 14, [6], 927-30 (1962).(English translation).

28. Ye. S. Borovik and N. G. Yakovleva, "Magnetic Properties of Binary Systems of Mixed Lead-Barium and Lead-Strontium Ferrites", Fiz. Metal. Metalloved., 15, [1], 151-53 (1963). (English translation).

29. P. Hutny, "Permanent Magnets of Barium Strontium Ferrites", Fiz. Metal. Metalloved., 16, [1], 132-33 (1963). (English translation).

30. J. W. Bergstrom, "General Motors Ferriroll Process", Paper presented at the Annual Meeting of the Canadian Ceramic Society, February, 1967.

31. H. J. Van Hook, "Thermal Stability of Barium Ferrite ($BaFe_{12}O_{19}$)", J. Am. Ceram. Soc., 47, [11], 579-81 (1964).

32. W. S. Clabaugh, E. M. Swiggard and R. Gilchrist, "Preparation of Barium Titanyl Oxalate Tetrahydrate for Conversion to Barium Titanate of High Purity", J. Research Nat. Bur. Stds., 56, [5], 289-91 (1956).

33. P. K. Gallagher, "Thermal Decomposition of Barium and Strontium Trisoxalatoferrates (III)", Inorg.Chem., 4, [7], 965-940 (1965).

34. J. F. Wenckus and W. Z. Leavitt, "Preparation of Ferrites by the Atomizing Burner Technique", Paper presented at the Conference on Magnetism and Magnetic Materials in Boston, 1956.

- - -

APPENDIX III

ELECTRONIC CERAMICS
ECRDC RESEARCH PROJECT C 73

Identification of Mines Branch Personnel

Advisory Committee

Mr. Ian F. Wright, MPD*, Chairman
Mr. W.A. Gow, EMD
Dr. N.F.H. Bright, MSD
Mr. J.G. Brady, MPD
Mr. V.A. McCourt, MPD

Operational

Mr. V.M. McNamara, EMD	Pilot plant ceramic powder preparation
Mr. J.C. Ingles, EMD	Control analyses
Dr. A.H. Webster, MSD	Sintering and structural studies
Mr. V.A. McCourt, MPD	Lapidary and electroding
Mr. Ian F. Wright, MPD	Ceramic engineering
Mr. T.B. Weston, MPD	Electronic test methods and component evaluation
Mr. W.R. Inman, MSD	Wet chemical analytical methods and analyses
Dr. A.H. Gillieson, MSD	Spectrographic analyses
Dr. E.H. Nickel, MSD	Sample preparation for petrographic studies

*MPD - Mineral Processing Division
EMD - Extraction Metallurgy Division
MSD - Mineral Sciences Division

Ian F. Wright
Project Co-ordinator

John Convey
Director, Mines Branch